CHEMISTRY
A EUROPEAN JOURNAL

DOI: 10.1002/chem.200600679

Oxo- and Imidovanadium Complexes Incorporating Methylene- and Dimethyleneoxa-Bridged Calix[3]- and -[4]arenes: Synthesis, Structures and Ethylene Polymerisation Catalysis

Carl Redshaw,*[a] Michael A. Rowan,[a] Lee Warford,[a] Damien M. Homden,[a] Abdessamad Arbaoui,[a] Mark R. J. Elsegood,[b] Sophie H. Dale,[b] Takehiko Yamato,[c] Carol Pérez Casas,[c] Shigekazu Matsui,[d] and Sadahiko Matsuura[d]

Abstract: Reaction of $[V(X)(OR)_3]$ (X = O, N*p*-tolyl; R = Et, *n*Pr or *t*Bu) with *p-tert*-butylhexahomotrioxacalix[3]areneH_3, LH_3, affords the air-stable complexes $[\{V(X)L\}_n]$ (X = O, $n = 1$ (**1**); X = N*p*-tolyl, $n = 2$ (**2**)). Alternatively, **1** is readily available either from interaction of $[V(mes)_3THF]$ with LH_3, and subsequent oxidation with O_2 or upon reaction of LLi_3 with $[VOCl_3]$. Reaction of $[V(Np\text{-tolyl})(OtBu)_3]$ with 1,3-dimethylether-p-*tert*-butylcalix[4]areneH_2, $Cax(OMe)_2(OH)_2$, afforded $[\{VO(OtBu)\}_2(\mu\text{-}O)Cax(OMe)_2(O)_2]\cdot 2MeCN$ (**4**·2MeCN), in which two vanadium atoms are bound to just one calix[4]arene ligand; the *n*-propoxide analogue of **4**, namely $[\{VO(OnPr)\}_2(\mu\text{-}O)Cax(OMe)_2(O)_2]\cdot 1.5MeCN$ (**5**·1.5MeCN), has also been isolated from a similar reaction using $[V(O)(OnPr)_3]$. Reaction of $[VOCl_3]$, $LiOtBu$, $(Me_3Si)_2O$ and $Cax(OMe)_2(OH)_2$ gave $[\{VO(OtBu)Cax(OMe)_2(O)_2\}_2Li_4O_2]\cdot 8MeCN$ (**6**·8MeCN), in which an Li_4O_4 cube (two of the oxygen atoms are derived from the calixarene ligands) is sandwiched between two $Cax(OMe)_2(O)_2$. The reaction between $[V(Np\text{-tolyl})(OtBu)_3]$ and $Cax(OMe)_2(OH)_2$, afforded $[V(Np\text{-tolyl})(OtBu)_2Cax(OMe)_2(O)(OH)]\cdot 5MeCN$ (**7**·5MeCN), in which two *tert*-butoxide groups remain bound to the tetrahedral vanadium atom, which itself is bound to the calix[4]arene through only one phenolic oxygen atom. Reaction of p-*tert*-butylcalix[4]areneH_4, $Cax(OH)_4$ and $[V(Np\text{-tolyl})(OnPr)_3]$ led to loss of the imido group and formation of the dimeric complex $[\{VCax(O)_4(NCMe)\}_2]\cdot 6MeCN$ (**8**·6MeCN). Monomeric vanadyl oxo- and imidocalix[4]arene complexes $[V(X)Cax(O)_3(OMe)(NCMe)]$ (X = O (**11**), N*p*-tolyl (**12**)) were obtained by the reaction of the methylether-p-*tert*-butylcalix[4]areneH_3, $Cax(OMe)(OH)_3$, and $[V(X)(OR)_3]$ (R = Et or *n*Pr). Vanadyl calix[4]arene fragments can be linked by the reaction of 2,6-bis(bromomethyl)pyridine with $Cax(OH)_4$ and subsequent treatment with $[VOCl_3]$ to afford the complex $[\{VOCax(O)_4\}_2(\mu\text{-}2,6\text{-}(CH_2)_2C_5H_3N)]\cdot 4MeCN$ (**13**·4MeCN). The compounds **1**–**13** have been structurally characterised by single-crystal X-ray diffraction. Upon activation with methylaluminoxane, these complexes displayed poor activities, however, the use of dimethylaluminium chloride and the reactivator ethyltrichloroacetate generates highly active, thermally stable catalysts for the conversion of ethylene to, at 25 °C, ultra-high-molecular-weight (> 5500000), linear polyethylene, whilst at higher temperature (80 °C), the molecular weight of the polyethylene drops to about 450000. Using **1** and **2** at 25 °C for ethylene/propylene co-polymerisation (50:50 feed) leads to ultra-high-molecular-weight (> 2900000) polymer with about 14.5 mol % propylene incorporation. The catalytic systems employing the methyleneoxa-bridged complexes **1** and **2** are an order of magnitude more active than the bimetallic complexes **5** and **13**, which, in turn, are an order of magnitude more active than pro-catalysts **8**, **11** and **12**. These differences in activity are discussed in terms of the structures of each class of complex.

Keywords: calixarenes · ethylene · polymerization · vanadium

[a] Dr. C. Redshaw, M. A. Rowan, L. Warford, D. M. Homden, A. Arbaoui
Wolfson Materials and Catalysis Centre
School of Chemical Sciences and Pharmacy
University of East Anglia, Norwich, NR4 7TJ (UK)
Fax: (+44) 1603-593-137
E-mail: carl.redshaw@uea.ac.uk

[b] Dr. M. R. J. Elsegood, S. H. Dale
Chemistry Department, Loughborough University
Loughborough, Leicestershire, LE11 3TU (UK)

[c] Prof. T. Yamato, C. P. Casas
Department of Applied Chemistry
Faculty of Science and Engineering, Saga University
Honjo-machi 1, Saga-shi, 840–8502 (Japan)

[d] Dr. S. Matsui, S. Matsuura
R & D Centre, Mitsui Chemical Inc.
580–32 Nagaura, Sodegaura, Chiba 299–0265 (Japan)

Introduction

During the past decade, interest in the coordination chemistry of calixarenes has increased year on year. This interest stems from its many applications, such as medical diagnostics, sensors and phase-transfer agents.[1] However, their use in polymerisation catalysis has only recently gained attention. Zheng et al. have utilised calixarene systems in both polystyrene and polypropylene oxide synthesis,[2a] and Shen et al. have used rare-earth calixarenes to initiate the ring-opening polymerisation of 2,2-dimethyltrimethylene carbonate,[2b] whilst Ladipo et al.,[2c] Proto et al.,[2d] Shen et al.[2e] and ourselves[2f] have had limited success with polyethylene (reported activities $<100\,g\,mmol^{-1}\,h^{-1}\,bar^{-1}$). Very recently, Kim and co-workers have reported that mixtures of a chromium(III) calix[4]arene of unknown structure with alkylaluminium co-catalysts, polymerises ethylene with activities as high as $1500\,g\,mmol^{-1}\,h^{-1}$ (at 35 bar) to afford polyethylene with low average molecular weight (910–9740).[2g] Interestingly, Floriani and co-workers have found that cationic zirconium calix[4]arenes are inactive towards olefin polymerisation.[2h] Calixarenes, in conjunction with dibutylphthalate, have also been used as selectivity control agents in Ziegler–Natta polypropylene catalysis.[2i] Reports in the patent literature concerning the use of calixarenes in olefin polymerisation are also scant.[3]

Our interest in developing new catalytic systems containing calixarene ligands has led us to discover a new class of pro-catalyst based on oxo- or organoimidovanadium(V) centres supported by the hexahomotrioxacalix[3]arene ligand, LH_3, and offer scope for polymerisation applications extending beyond α-olefins. In contrast to the rich transition-metal coordination chemistry known for methylene(-CH_2-)-bridged calix[*n*]arenes,[4] the related dimethyleneoxa(-CH_2OCH_2-)-bridged oxacalix[*n*]arenes have received very little attention.[5] Here, we report the synthesis and structures of the complexes [V(O)L] (**1**) and [{V(N*p*-tolyl)L}$_2$] (**2**) (where L is the deprotonated from of p-*tert*-butylhexahomotrioxacalix[3]arene), and results of catalytic screening studies for polyethylene (and for ethylene/propylene copolymerisation), which reveal, for this metal, phenomenal activities. We have also prepared and structurally characterised a number of unusual calix[4]arene derived complexes, and we have tested representative examples so that comparisons can be made between the two series, namely calixarenes versus oxacalixarenes. Vanadium-based catalysts though used commercially usually suffer from intrinsically low activities compared to Group IV systems, due mainly to catalyst deactivation/reduction to inactive states.[6] In the patent literature, there are numerous discussions of the use/potential of vanadyl alkoxides/aryloxides, in combination with organoaluminium reagents, for olefin polymerisation;[7a] however, the use of related organoimido species is far less common.[7b] The potential of vanadium-based systems has been highlighted recently by a number of groups (Scheme 1). Fujita et al. utilised phenoxyimine-type complexes **I** heterogenised on $MgCl_2$-based surfaces, Gibson et al. have used bis(benzimidazole)amine complexes **II**, Nomura et al. have had success with aryl oxides of the form [V(N-2,6-$R_2C_6H_3$)(OAr)Cl_2] (**III**; R = Me, *i*Pr; Ar = 2,6-$Me_2C_6H_3$, 2,6-*i*$Pr_2C_6H_3$, 2,6-$Ph_2C_6H_3$), and we have shown that the bi- (**IV**) and tri- (**V**) phenolate vanadyl complexes are highly active upon activation with dimethylaluminium chloride (DMAC).[8]

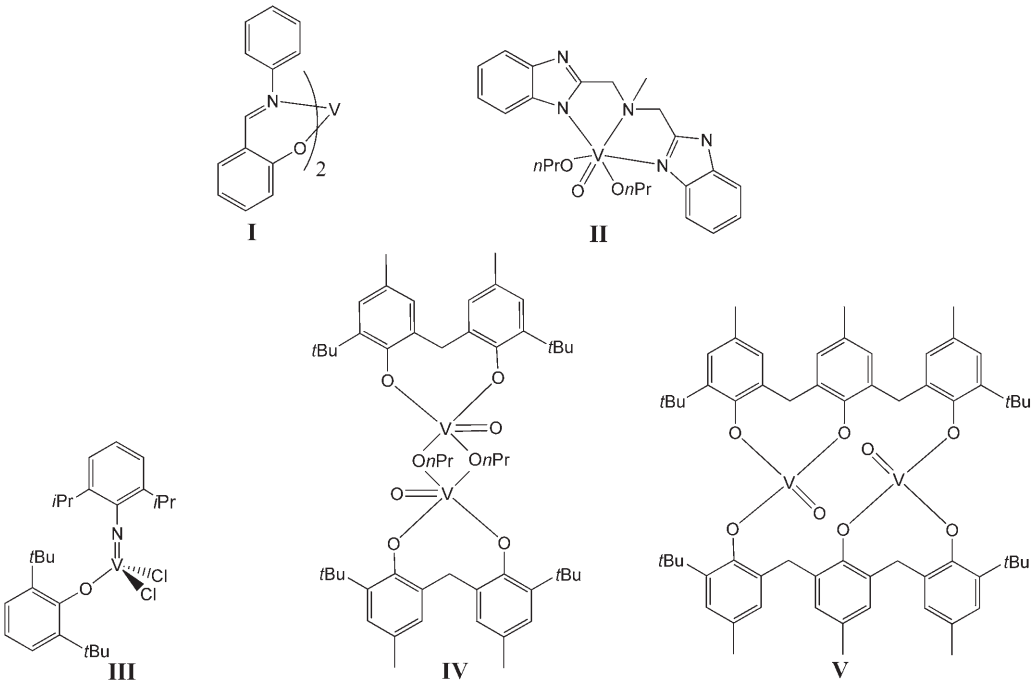

Scheme 1. Highly active vanadium-based pro-catalysts.

Results and Discussion

Oxacalix[3]arene complexes: The oxo- and organoimido-oxacalix[3]arene pro-catalysts used in this study can be prepared in good yield, as yellow to orange air-stable solids, from the reaction of the alkoxides $[V(O)(OR)_3]$ and $[V(N\text{-}p\text{-tolyl})(OR)_3]_2$ (R = Et, *n*Pr, *t*Bu) and the parent LH_3, respectively. Alternatively, the pro-catalysts can be prepared by the use of the lithium salts Li_3L and the metal chlorides $[VOCl_3]$ and $[V(Np\text{-tolyl})Cl_3]$, respectively, or in the case of **1**, by the interaction of the tris(mesityl)vanadium(III) complexes $[V(mes)_3(THF)]$ (mes = 2,4,6-$Me_3C_6H_3$) or $[VCl_3(THF)_3]$ (in the presence of Et_3N) with the parent LH_3 ligand followed by reaction with dry oxygen (Scheme 2).

Crystals of the oxo pro-catalyst **1a** suitable for an X-ray determination, which were prepared via the $[VO(OnPr)_3]$ route, were obtained by slow evaporation of the acetonitrile solvent under air. The complex (Figure 1) is monomeric with a trigonal-pyramidal vanadium atom, and contrasts with the μ-oxo-bridged linear chain polymer observed (by IR and ^{51}V NMR spectroscopy and X-ray powder diffraction) for $[V(O)L^1]$(L^1=triply deprotonated *p*-methylhexahomotrioxacalix[3]arene).[5b] The V=O distance (1.572(3) Å) is typical,[9] and a strong band in the IR spectrum at 1014 cm^{-1} is assigned to this grouping. The molecular weight determined cryoscopically was 706 (calcd 640), which indicated

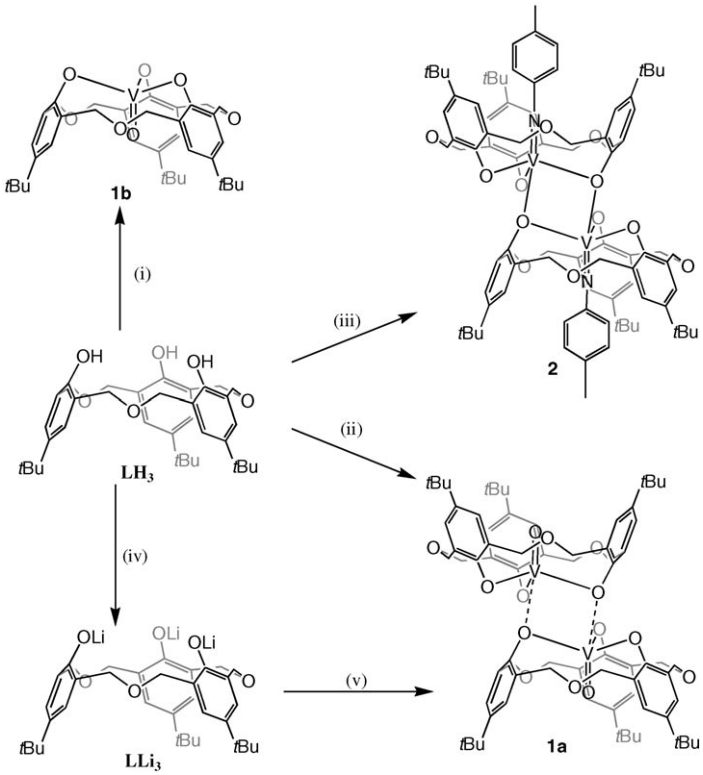

Scheme 2. Synthesis of LLi_3, **1a**,**b** and **2**. i) 1. $[V(mes)_3(THF)]$, THF, −78 °C, 2 h, 2. O_2, 25 °C, 5 min; ii) $[V(O)(OnPr)_3]$, toluene, 60 °C, 2 h; iii) $[V(Np\text{-tolyl})(OEt)_3]$, toluene, 60 °C, 2 h; iv) 3 MeLi, −78 °C, 2 h; v) $[VOCl_3]$.

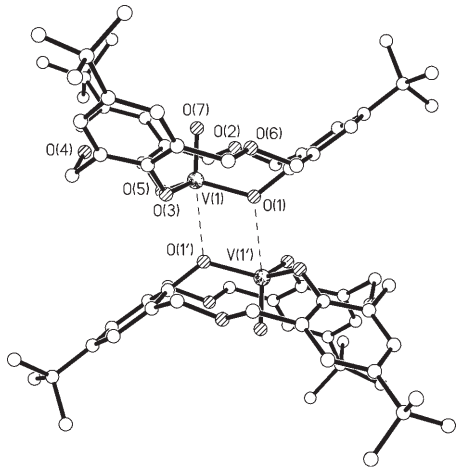

Figure 1. Weakly associated pairs of molecules in the crystal structure of **1a**. Selected bond lengths [Å] and angles [°]: V(1)–O(1) 1.848(2), V(1)–O(3) 1.805(2), V(1)–O(7) 1.572(2), O(1)–V(1′) 2.473(2); O(1)-V(1)-O(1′) 111.2(11).

an association constant of 1.1, and the molecular ion was observed by electrospray mass spectrometry.

However, in the solid-state there are very weak interactions between O(1) and V(1′) (on a neighbouring molecule) at 2.473 Å. This gives rise to a pair of molecules lying face-to-face over an inversion centre. There is one acetonitrile per molecule of the complex, which sits just within the rim of the bowl. Bowls from two neighbouring molecules slightly interlock and encapsulate two acetonitrile molecules. Crystallographic data are presented in Table 1.

Surprisingly, the crystal structure determined by using synchrotron radiation,[10] of the complex resulting from the $[V(mes)_3(THF)]/O_2$ route is somewhat different. Here for **1b**, the molecule is a discrete monomer with a mirror plane passing through V(1), O(3), O(4), O(5), C(13) and C(17) (Figure 2a). The geometry at the vanadium atom now approaches tetrahedral, whilst the V–O bond lengths here are essentially the same as those noted above for **1a**. However, there is no incorporation of solvent (MeCN). Interestingly, the molecules simply stack in columns parallel to the *a* axis, with neighbouring columns in the *c* direction aligned the same way, while neighbours in the *b* direction are aligned in opposite directions (see Figure 2b). This same complex can also be obtained by treatment of the parent LH_3 with 3.2 equivalents of MeLi and subsequent addition of $[VOCl_3]$.

We believe that the encapsulation of the oxo (vanadyl) group by the macrocycle leaves the four-coordinate, coordinatively unsaturated vanadium atom exposed (see space-filling diagram, Figure 3), and renders it more susceptible to alkylation by DMAC, ultimately resulting in the observed high activity.

Solution NMR data for **1a** and **1b** suggest the same structure is adopted in solution for both.

Crystals of the imido pro-catalyst **2**, obtained via $[V(N\text{-}p\text{-tolyl})(OtBu)_3]$, suitable for an X-ray diffraction study (Figure 4) were grown from acetonitrile at ambient tempera-

Table 1. Crystallographic data.

Compound	**1a**·MeCN	**1b**	**2**·5 MeCN	**3**	**4**·2 MeCN	**5**·1.125 MeCN	**6**
formula	$C_{38}H_{48}NO_7V$	$C_{36}H_{45}O_7V$	$C_{96}H_{119}N_7O_{12}V_2$	$C_{38}H_{51}NO_6$	$C_{58}H_{82}N_2O_9V_2$	$C_{54.5}H_{75.75}N_{1.25}O_9V_2$	$C_{116}H_{158}Li_4N_8O_{14}V_2$
formula weight	681.71	640.66	1664.86	617.80	1053.14	994.29	2018.14
crystal system	triclinic	monoclinic	triclinic	orthorhombic	orthorhombic	orthorhombic	triclinic
space group	$P\bar{1}$	$P2_1/m$	$P\bar{1}$	$Pca2_1$	*Pnma*	*Pnma*	$P\bar{1}$
unit cell dimensions							
a [Å]	11.4462(10)	9.663(3)	11.7980(15)	22.146(4)	26.2908(12)	26.070(5)	13.5282(13)
b [Å]	12.2963(11)	17.031(5)	13.7892(17)	17.253(4)	16.3974(7)	15.906(3)	20.012(2)
c [Å]	15.5971(13)	10.229(3)	15.2655(19)	9.3682(19)	13.7049(6)	13.569(3)	21.996(2)
α [°]	67.415(2)	90	86.059(2)	90	90	90	100.202(4)
β [°]	75.808(2)	101.900(6)	73.260(2)	90	90	90	100.952(4)
γ [°]	62.408(2)	90	79.096(2)	90	90	90	91.272(4)
V [Å^3]	1790.3(3)	1647.3(8)	2335.0(5)	3579.4(12)	5908.2(5)	5626.6(19)	5744.4(10)
Z	2	2	1	4	4	4	2
T [K]	150(2)	150(2)	150(2)	120(2)	150(2)	150(2)	150(2)
radiation, λ [Å]	sealed tube, 0.71073	synchrotron, 0.6895	sealed tube, 0.71073	rotating anode, 0.71073	sealed tube, 0.71073	synchrotron, 0.8464	sealed tube, 0.71073
ρ_{calcd} [g cm^{-3}]	1.265	1.292	1.184	1.146	1.184	1.174	1.167
absorption coefficient [mm^{-1}]	0.326	0.348	0.261	0.076	0.369	0.383	0.225
crystal size [mm]	0.36×0.14×0.05	0.10×0.06×0.03	0.65×0.41×0.39	0.20×0.04×0.02	0.40×0.40×0.39	0.10×0.09×0.02	0.53×0.16×0.10
$2\theta_{max}$ [°]	50.0	59.0	57.8	45.0	55.0	50.0	50.0
reflections measured	16202	12795	20239	13695	49415	16807	41257
unique reflections	6304	4719	10652	4365	6985	3060	19577
reflections with $F^2>2\sigma(F^2)$	4057	4141	9086	2330	5380	2033	11185
transmission factors	0.89–0.98	0.97–0.99	0.85–0.91	0.81–0.84	0.86–0.87	0.96–0.99	0.89–0.98
R_{int}	0.0520	0.0313	0.0213	0.1571	0.0267	0.1041	0.0788
number of parameters	459	226	627	442	388	380	1376
R[a] [$F^2>2\sigma(F^2)$]	0.0502	0.0532	0.0605	0.0751	0.0584	0.0720	0.0680
R_w[b] (all data)	0.1366	0.1580	0.1810	0.1850	0.1653	0.1987	0.2012
largest difference peak and hole [e Å^{-3}]	0.503 and −0.562	1.14 and −0.46	1.275 and −0.628	0.211 and −0.178	0.732 and −0.563	0.472 and −0.288	0.599 and −0.522

Compound	**7**	**8**	**9**·MeCN	**10**·2 MeCN	**11**·2.5 MeCN	**12**·1.125 MeCN	**13**
formula	$C_{71}H_{99}N_6O_6V$	$C_{104}H_{128}N_8O_8V_2$	$C_{94}H_{113}N_3O_8V_2$	$C_{96}H_{116}N_4O_8V_2$	$C_{50}H_{62.5}N_{2.5}O_5V$	$C_{54.25}H_{65.375}N_{2.125}O_4V$	$C_{103}H_{123}N_5O_{10}V_2$
formula weight	1183.50	1720.02	1514.76	1555.81	829.47	862.15	1692.94
crystal system	triclinic	orthorhombic	monoclinic	monoclinic	orthorhombic	triclinic	monoclinic
space group	$P\bar{1}$	*Pbca*	$P2_1/c$	$P2_1/c$	*Pbcn*	$P\bar{1}$	$P2_1/n$
unit cell dimensions							
a [Å]	14.1777(6)	21.5081(13)	10.8599(7)	17.065(2)	14.7161(17)	21.6027(8)	13.6545(7)
b [Å]	14.7627(6)	18.8533(12)	23.8714(15)	19.444(3)	26.721(3)	21.7462(8)	31.0602(16)
c [Å]	17.3826(8)	24.2673(15)	16.6908(11)	13.4761(18)	23.299(3)	21.8257(8)	22.9153(12)
α [°]	77.852(2)	90	90	90	90	90.788(2)	90
β [°]	80.344(2)	90	103.428(2)	96.722(2)	90	102.047(2)	91.344(2)
γ [°]	88.382(2)	90	90	90	90	99.485(2)	90
V [Å^3]	3506.2(3)	9840.4(11)	4208.7(5)	4440.7(10)	9161.9(18)	9878.0(6)	9716.0(9)
Z	2	4	2	2	8	8	4
T [K]	150(2)	150(2)	150(2)	150(2)	120(2)	120(2)	150(2)
radiation, λ [Å]	sealed tube, 0.71073	sealed tube, 0.71073	synchrotron, 0.6861	synchrotron, 0.6861	synchrotron, 0.6897	synchrotron, 0.6861	sealed tube, 0.71073
ρ_{calcd} [g cm^{-3}]	1.121	1.161	1.195	1.164	1.203	1.159	1.157
absorption coefficient [mm^{-1}]	0.193	0.248	0.279	0.266	0.264	0.246	0.250
crystal size [mm]	0.43×0.37×0.12	0.74×0.53×0.27	0.20×0.03×0.03	0.08×0.06×0.02	0.19×0.17×0.04	0.13×0.10×0.07	0.41×0.15×0.08
$2\theta_{max}$ [°]	55.0	58.0	58.7	52.0	61.9	50.0	50.0
reflections measured	30553	81448	43318	26447	104880	83775	70407
unique reflections	15642	12209	12032	9658	15209	37930	17112
reflections with $F^2>2\sigma(F^2)$	10084	8520	9687	5938	11352	26159	9612
transmission factors	0.92–0.98	0.84–0.94	0.95–0.99	0.98–0.99	0.95–0.99	0.97–0.98	0.90–0.98
R_{int}	0.0321	0.0539	0.0374	0.0568	0.0654	0.0511	0.0698
number of parameters	786	597	524	561	575	2547	1186
R[a] [$F^2>2\sigma(F^2)$]	0.0498	0.0706	0.0447	0.0585	0.0726	0.1060	0.0723
R_w[b] (all data)	0.1449	0.2474	0.1275	0.1678	0.1688	0.2423	0.2436
largest difference peak and hole [e Å^{-3}]	0.435 and −0.437	0.886 and −0.582	0.574 and −0.523	0.592 and −0.547	1.084 and −1.005	2.679 and −2.453	0.839 and −0.450

[a] Conventional $R=\Sigma||F_o|-|F_c||/\Sigma|F_o|$ for "observed" reflections having $F^2>2\sigma(F^2)$. [b] $R_w=[\Sigma w(F_o^2-F_c^2)^2/\Sigma_w(F_o^2)^2]^{1/2}$ for all data. [c] $S=[\Sigma w(F_o^2-F_c^2)^2/(\text{no. of unique reflections}-\text{no. of parameters})]^{1/2}$.

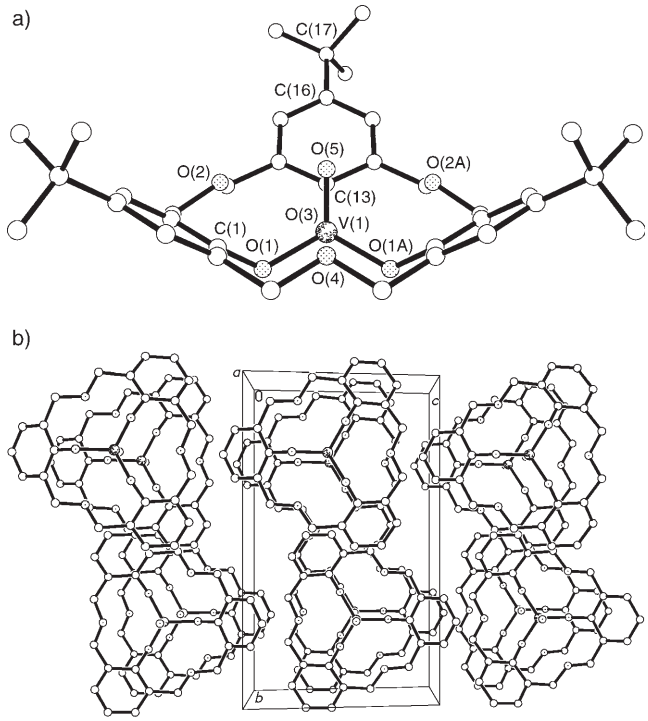

Figure 2. a) Molecular structure of **1b**, which lies on a mirror plane. Selected bond lengths [Å]: V(1)–O(1) 1.8027(13), V(1)–O(3) 1.8052(19), V(1)–O(5) 1.5662(18). b) Packing of **1b** with *t*Bu groups omitted for clarity.

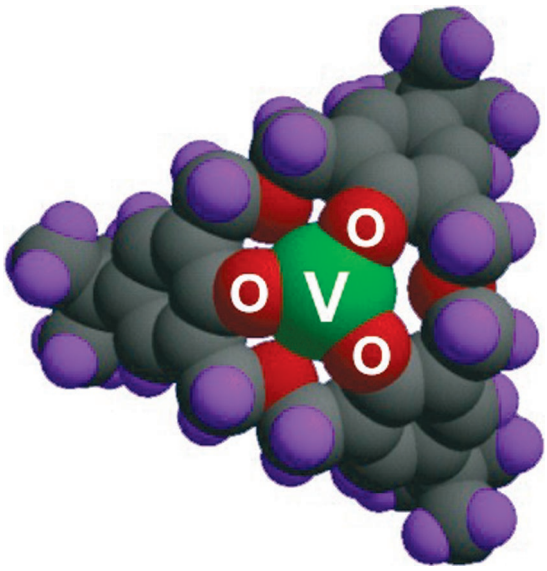

Figure 3. Space-filling diagram of **1b** clearly showing the exposed face of vanadium.

ture: they incorporate five molecules of solvent per molecule of the complex. The molecule is a centrosymmetric dimer, with asymmetric "phenoxide" bridges, and in which each vanadium atom is trigonal-bipyramidal. The longer

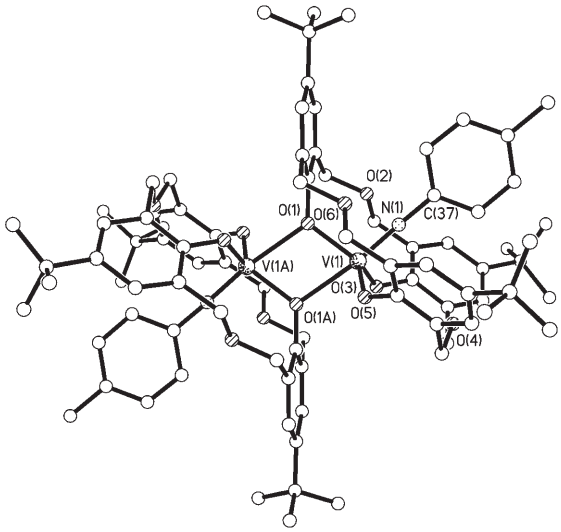

Figure 4. Molecular structure of **2**. Selected bond lengths [Å] and angles [°]: V(1)–O(1A) 2.3017(16), V(1)–O(1) 1.8922(17), V(1)–O(3) 1.8316(18), V(1)–O(5) 1.8312(17), V(1)–N(1) 1.652(2); V(1)-O(1)-V(1A) 108.38(7), V(1)-N(1)-C(37) 178.12(19).

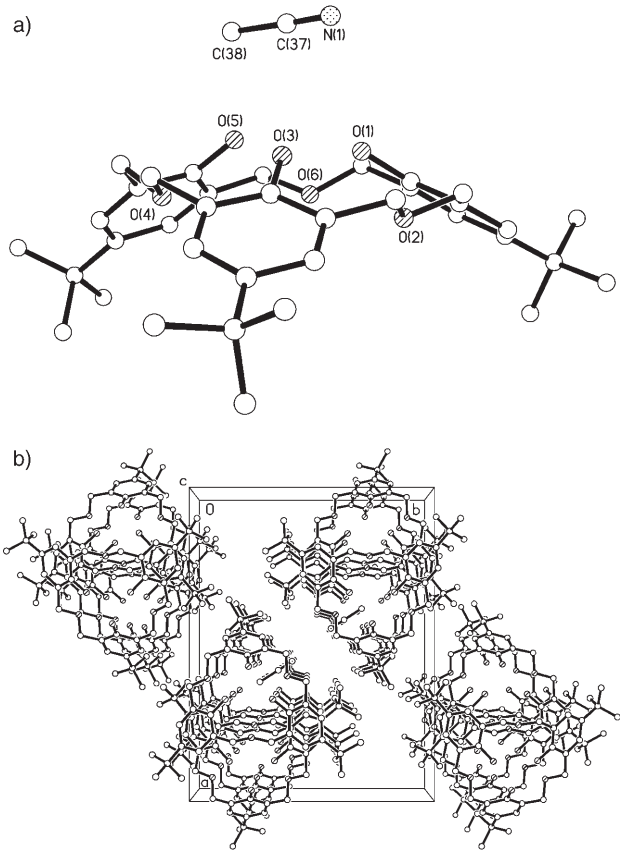

Figure 5. a) Molecular structure of **3**. Selected bond lengths [Å] and angles [°]: O(1)–C(1) 1.392(9), O(2)–C(12) 1.437(8), O(2)–C(11) 1.448(8), O(5)–H(38C) 2.56, O(1)–C(37) 4.330, O(3)–C(37) 3.305, O(5)–C(38) 3.514; C(12)-O(2)-C(11) 115.5(5), C(6)-C(1)-O(1) 122.1(7). b) Packing of **3** in stacked columns.

bridging bond is *trans* to a near-linear *p*-tolylimido group, the latter residing within the oxacalix[3]arene cavity.

For the ^{51}V NMR spectrum of **2**, the line width is greater than that of **1a,b** (1998 compared with 143 Hz), whilst the chemical shift is somewhat downfield ($\delta = -209.2$ compared with $\delta = -321.3$ ppm for **1**); a trend noted previously by Maatta et al.[11]

We have structurally characterised LH_3 as its acetonitrile solvate. The geometrical parameters associated with the cone conformation of LH_3 observed here are basically the same as those reported for a solvent-free sample recrystallised from *m*-xylene.[12] In LH_3·MeCN (**3**) the molecules form stacks with successive molecules slipped with respect to those above and below. The solvent molecules (MeCN) fill the gaps between molecules in the stacks (see Figure 5a and b).

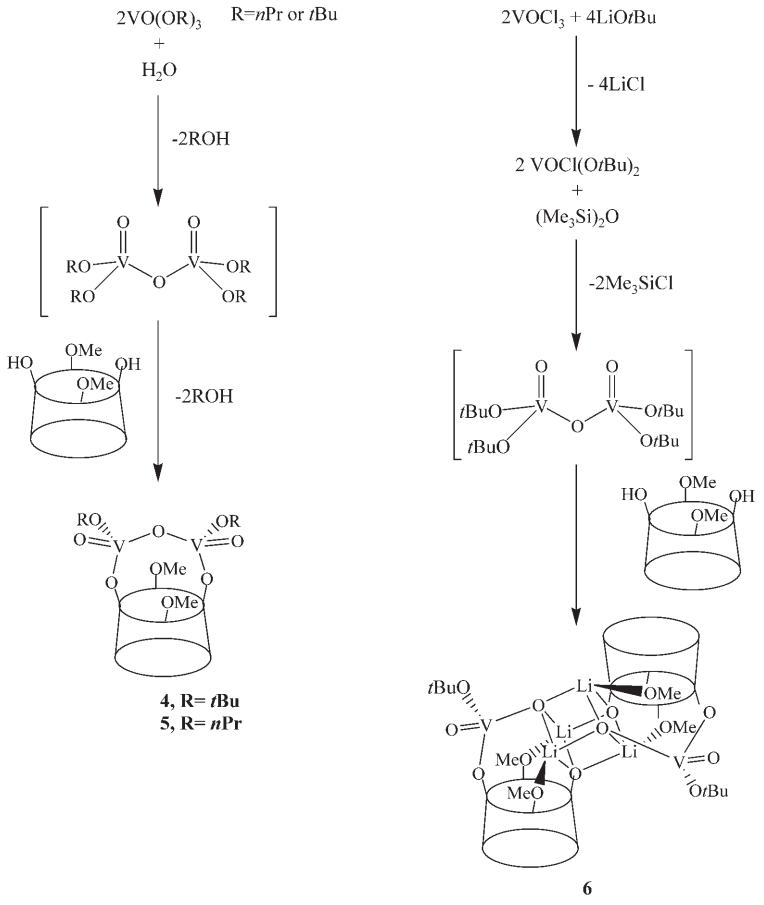

Scheme 3. Synthesis of the vanadium complexes **4, 5** and **6**.

Calix[4]arene complexes: Calix[4]arenes can also be used as polyoxo supports for vanadium, and a number of V^{III}, V^{IV} and V^{V} species have been reported by the groups of Floriani[13a,b] and Limberg.[13c] None of these species were, however, investigated as potential catalysts for α-olefin polymerisations. Our initial investigations focused on the reaction of the oxo and imido *tert*-butoxide starting materials [V(X)-(O*t*Bu)$_3$] (X = O or N*p*-tolyl) with 1,3-dimethylether-p-*tert*-butylcalix[4]arene, [Cax(OMe)$_2$(OH)$_2$] (see Scheme 3).

Following reaction of [Cax(OMe)$_2$(OH)$_2$] with [V(O)-(O*t*Bu)$_3$] in refluxing toluene, small orange prisms were formed on work-up and extraction into acetonitrile. A single-crystal X-ray analysis (Figure 6) of these weakly diffracting prisms shows that two vanadium atoms are bound to one Cax(OMe)$_2$(O)$_2$ ligand, each through a single calixarene oxygen atom to afford {[VO(O*t*Bu)]$_2$(μ-O)Cax-(OMe)$_2$(O)$_2$}·2MeCN (**4**·2MeCN).

The two pseudo-tetrahedral vanadium atoms are linked together through a μ-oxo bridge and the molecule of **4** lies on a mirror plane. The vanadyl V(1)–O(6) bond length (1.594(2) Å) is similar to those observed in both versions of **1** (1.572(2) and 1.5662(18) Å) and to that reported for the related calix[4]arene complex [VOCax(O)$_3$(OMe)],[13] whilst as expected the bridging oxo distances (1.7805(1) Å) are slightly longer. The *tert*-butoxide ligand is bent (135.6°), which reflects the competitive π-donation to the metal centre. There are two solvent molecules (MeCN) per molecule of **4**; one MeCN resides inside the Cax(OMe)$_2$(O)$_2$ cone, the other is below it and slightly off-set to one side.

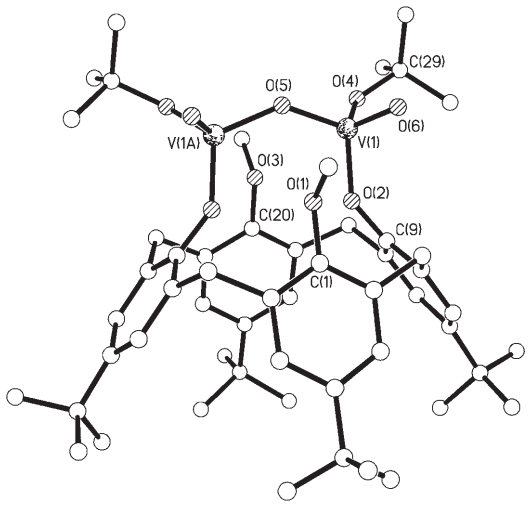

Figure 6. Molecular structure of **4**. Selected bond lengths [Å] and angles [°]: V(1)–O(5) 1.7805(11), V(1)–O(6) 1.594(2), V(1)–O(4) 1.747(2), V(1)–O(2) 1.7630(19); V(1)-O(5)-V(1A), 138.01(17), V(1)-O(4)-C(1) 135.6(2).

Similar use of $[V(O)(OnPr)_3]$ and $Cax(OH)_2(OMe)_2$ readily yields the *n*-propoxide analogue of **4**, namely $\{[VO(OnPr)]_2(\mu\text{-}O)Cax(OMe)_2(O)_2\}$ (**5**) as orange-red prisms in about 40% yield. Crystals suitable for a structure determination using synchrotron radiation were grown from a saturated acetonitrile solution at ambient temperature. The structure of **5** (Figure 7) is similar to **4** with the $Cax(OMe)_2(O)_2$ ligand chelating to the same inorganic fragment, namely $\{[V(O)(OR)]_2(\mu\text{-}O)\}$. There is half a molecule of **5** and half an acetonitrile which are unique, and both lie on a mirror plane. There was evidence of another diffuse/partially occupied MeCN, which was modelled by using the Platon "squeeze" procedure to give an overall formula of **5**·1.25 MeCN. A molecule of acetonitrile resides within each $Cax(OMe)_2(O)_2$ cavity. The V=O (1.585(4) Å) and V−μ-O (1.771(2) Å) bond lengths are similar to those in **4** and, as in **4**, the alkoxide is considerably bent, though here they are somewhat different to one another (V(1)-O(2)-C(9) 148.4(4)° and V(1)-O(4)-C(29) 129.5(5)°), doubtless due to the packing of the molecule. Molecules of **5** align in alternate π–π-stacked chains affording a layer structure as shown in Figure 7b: along the *b* and *c* axes molecules alternate up, down, up, down, such that layers form in the *b*/*c* plane.

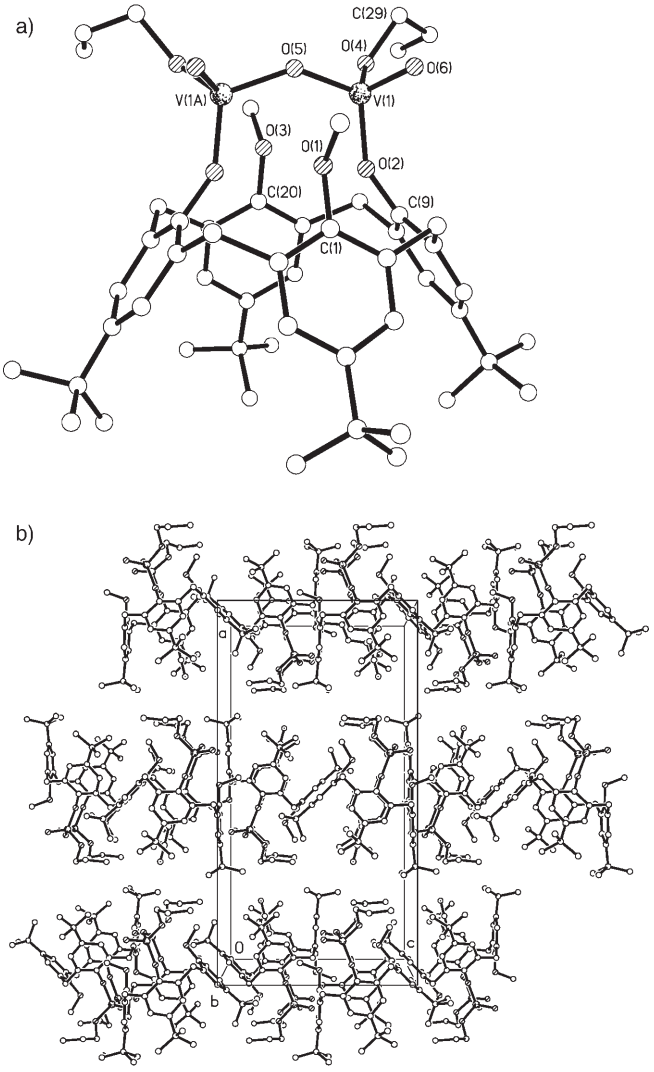

Figure 7. Molecular structure of **5**. Selected bond lengths [Å] and angles [°]: V(1)−O(2) 1.754(4), V(1)−O(4) 1.746(5), V(1)−O(5) 1.771(2), V(1)−O(6) 1.585(4); V(1)-O(5)-V(1A) 139.2(3), V(1)-O(2)-C(9) 148.4(4), V(1)-O(4)-C(29) 129.9(5).

Both **4** and **5** represent rare examples of complexes in which two metal centres are bound to a single calixarene ligand, the metal–metal separations V(1)···V(1A) are 3.325 and 3.319 Å, respectively.[4] The formation of **4** (and **5**) most likely involves a fortuitous hydrolysis reaction leading to the formation of an intermediate such as $\{[VO(OtBu)_2(\mu\text{-}O)\}$ (see Scheme 3a), formed via loss of *tert*-butyl alcohol. Further reaction with $Cax(OMe)_2(OH)_2$ leads to loss of two further equivalents of *tert*-butyl alcohol and formation of **4**. We envisaged that a more rational route might involve initial formation of a chloro-alkoxide of the form $[VOCl(OtBu)_2]$, to which we could introduce an oxo bridge by the use of the reagent $(Me_3Si)_2O$[14] (see Scheme 3b). Subsequent addition of $Cax(OMe)_2(OH)_2$ would then afford **4**. Following such a protocol in a "one-pot" procedure, a yellow product was isolated in about 60% yield. Recrystallisation from a saturated solution of acetonitrile at 0°C afforded pale yellow needles. The molecular structure of **6** (two views) is shown in Figure 8; there are also a total of eight acetonitrile molecules of crystallisation, two of which reside in the calix[4]arene cones. Interestingly, an Li_4O_4 cubane-type core has been trapped between two calix[4]arene units resulting in $[\{VO(OtBu)Cax(OMe)_2(O)_2\}_2Li_4O_2]\cdot 8\,MeCN$ (**6**·8 MeCN). When we consider that our aim here was to support the motif $\{[VO(OtBu)_2(\mu\text{-}O)\}$ found in **4**, the inorganic framework of **6** can be represented similarly as $\{[VO(OtBu)_2(\mu\text{-}Li_4O_4)\}$, which instead of being bound to just one calix[4]arene unit, rather prefers to bridge two.

Each vanadium atom in **6** is pseudo-tetrahedral with typical V=O bonds lengths (1.589(3) and 1.601(3) Å) and, as in **4**, is bound to significantly bent *tert*-butoxide groups (V-O-C 133.9(2) and 141.3(3)°). There are two different kinds of lithium centre: Li(1) and Li(4) are bound to two calixarene oxygen atoms and two μ_4 oxygen atoms in the cube, whilst Li(2) and Li(3) are bound to three calixarene oxygen atoms, and only one μ_4 oxygen atom in the cube. Each oxygen atom is therefore a μ_4 centre, with Li−O distances (1.843(8)–2.002(8) Å) similar to those described as short for the cubane system of $[Li_4Cax(O)_4(THF)_6]_2\cdot 6\,THF$.[15] This type of lithium–oxygen cubic core has also been observed in other transition-metal aryl oxide species,[16] and more recently has been highlighted as a possible building block in supramolecular chemistry.[17]

The reaction of $[V(Np\text{-tolyl})(OtBu)_3]$ with $Cax(OMe)_2(OH)_2$ was repeated under strictly anhydrous conditions (in the presence of activated molecular sieves). Crystallisation from a saturated acetonitrile solution on prolonged standing at ambient temperature afforded highly sol-

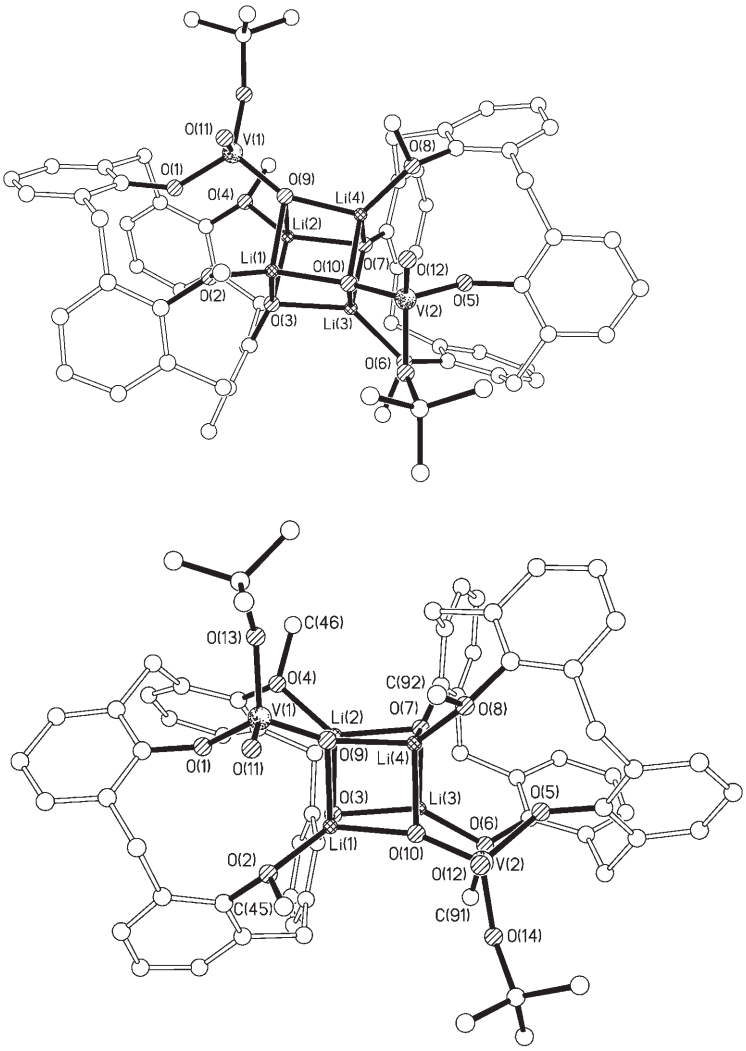

Figure 8. Molecular structure of **6**. Selected bond lengths [Å] and angles [°]: V(1)–O(1) 1.804(3), V(1)–O(9) 1.686(3), V(1)–O(11) 1.589(3), V(1)–O(13) 1.749(3), Li(1)–O(2) 1.867(7), Li(1)–O(3) 1.872(8), Li(2)–O(4) 1.898(8), Li(1)–O(9) 1.973(8), Li(1)–O(10) 1.929(8), Li(2)–O(3) 1.882(8), Li(2)–O(7) 1.987(8), Li(2)–O(9) 1.966(8); V(1)-O(13)-C(93), 141.3(3), V(1)-O(9)-Li(1), 113.9(2), V(1)-O(9)-Li(2), 118.8(3), O(9)-Li(1)-O(10), 93.6(3). Calixarene *tert*-butyl groups removed for clarity.

vent-dependent yellow-orange prisms of [V(N*p*-tolyl)-(O*t*Bu)$_2$Cax(OMe)$_2$(O)(OH)]·5MeCN (**7**·5MeCN) (see Scheme 4). The molecular structure of **7** is shown in Figure 9, for which there are five molecules of solvent (MeCN) per molecule of **7**, one of which resides in the calix-

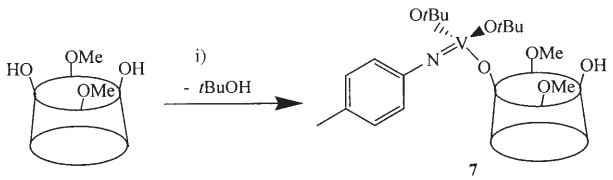

Scheme 4. Synthesis of the vanadium complex **7**. i) Toluene, reflux, 4 Å molecular sieves, 6 h.

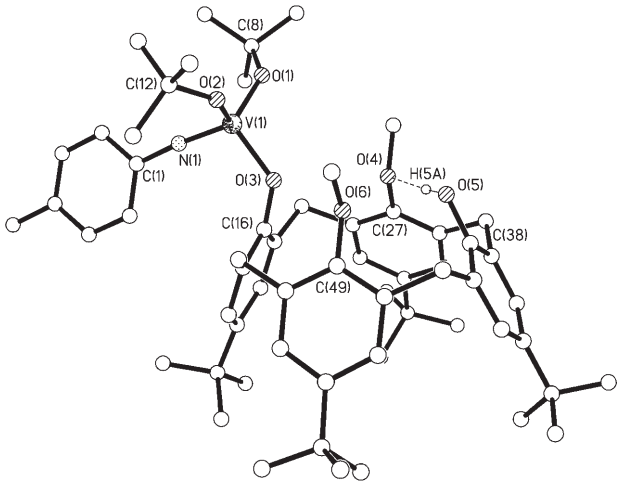

Figure 9. Molecular structure of **7**. Selected bond lengths [Å] and angles [°]: V(1)–O(1) 1.7725(16), V(1)–O(2) 1.7705(16), V(1)–O(3) 1.7978(15), V(1)–N(1) 1.6555(19); V(1)-O(1)-C(8) 139.49(15), V(1)-O(2)-C(12) 139.64(16), V(1)-O(3)-C(16) 129.91(13), V(1)-N(1)-C(1) 175.08(16).

arene cavity. Surprisingly, two *tert*-butoxide ligands are still bound to the vanadium atom, despite the presence of a "free" hydroxy group on the calix[4]arene lower-rim. The [V(N*p*-tolyl)(O*t*Bu)$_2$] fragment is bent away from the calixarene lower-rim (V(1)-O(3)-C(16) 129.91(13)°), whilst the "free" hydroxy group is involved in H-bonding with O(4) (O(5)···O(4) 2.737(2) Å).

In view of the structure of **7** and the suggestion that this represented an incomplete reaction, we reduced the steric bulk associated with each of the starting materials and reacted [V(N*p*-tolyl)(O*n*Pr)$_3$] with Cax(OH)$_4$. Following workup, recrystallisation from acetonitrile at ambient temperature afforded large red blocks in good yield (ca. 70%).

A single-crystal X-ray diffraction study (Figure 10, Table 1 and Table 2) revealed that the imido group had been lost,

Table 2. Bond lengths of **8**, **9**, **10** and [{VCax(O)$_4$}$_2$].

Complex	**8**	**9**	**10**	[{VCax(O)$_4$}$_2$]
V(1)–O(1)	1.892(2)	1.8742(10)	1.885(2)	1.835(5)
V(1)–O(2)	1.819(2)	1.8156(11)	1.8133(18)	1.742(5)
V(1)–O(3)	2.105(2)	2.1034(10)	2.102(2)	2.198(5)
V(1)–O(4)	1.819(2)	1.8170(11)	1.8064(18)	1.790(5)
V(1)–O(3′)	1.9091(18)	1.9039(10)	1.9026(18)	1.860(5)
V(1)–N(1)	2.159(2)	2.1683(13)	2.168(2)	–

resulting in the formation of the dimeric structure [{VCax(O)$_4$(NCMe)}$_2$]·6MeCN (**8**·6MeCN), closely related to the complex [V(Cax(O)$_4$)]$_2$ previously reported by Floriani et al.[13]

In the structure of **8**, there is half a molecule in the asymmetric unit together with three molecules of acetonitrile, the latter residing within voids in the lattice. The main difference between **8** and the structure reported by Floriani et al. is the presence of a metal-bound acetonitrile, and this results in two pseudo-octahedral vanadium atoms. The associ-

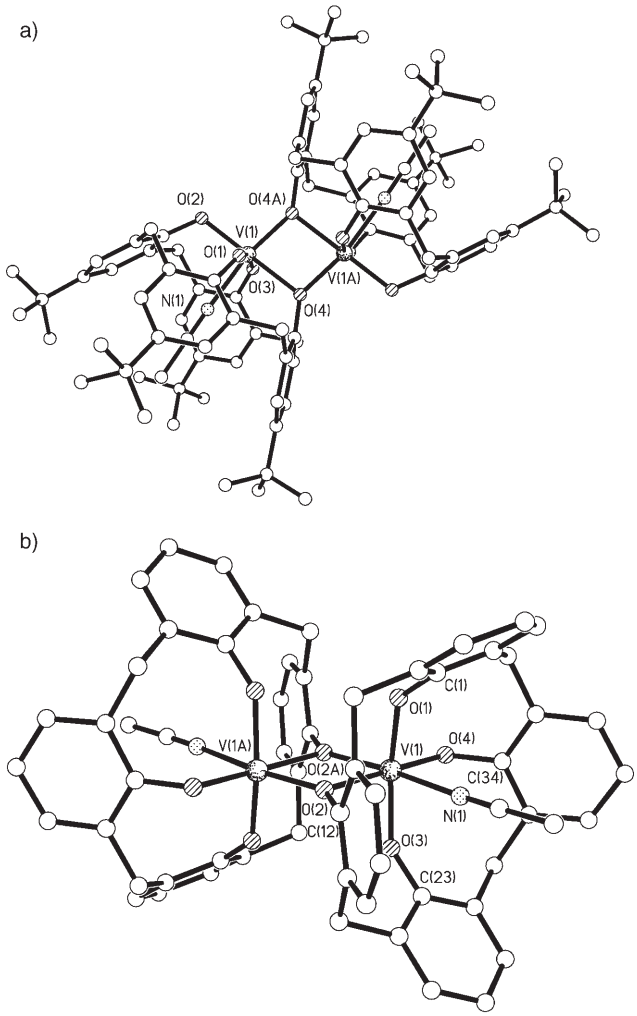

Figure 10. Crystal structures of a) **8** and b) **9** (with *tert*-butyl groups omitted), offering two alternative views. That of **10** is very similar.

ated V–O bonds are slightly longer than those in the structure described by Floriani et al. and this is thought to be due to the change from 5- to 6-coordination rather than any difference in oxidation state (the magnetic moment of **8** was found to be consistent with the presence of V^{IV} centres). Other solvates of **8** are also available (see Scheme 5) from the reaction of $K[V(OtBu)_4]$ (found in situ from $[VCl_3(THF)_3]$ and $KOtBu$) with $Cax(OH)_4$. Both small red needles and thin orange plates readily form on cooling a saturated solution to ambient temperature. Synchrotron radiation was used to establish the structural nature of each type of crystal, and revealed that the needles are $[\{VCax(O)_4(NCMe)\}_2]\cdot MeCN$ (**9**), whilst the plates are $[\{VCax(O)_4(NCMe)\}_2]\cdot 2MeCN$ (**10**). Selected structural parameters for **8**–**10** and $[VCax(O)_4]$ are presented in Table 2. Complexes **8**–**10** contain a central confacial bioctahedral structure, in which the bound solvent molecule occupies a position *trans* to the longest bridging bond.

Monomeric oxo- and imidovanadium calix[4]arene complexes were accessible (see Scheme 6) by the use of the tris(hydroxyl) ligand methylether-p-*tert*-butylcalix[4]areneH_3, $Cax(OMe)(OH)_3$, and $[VO(OnPr)_3]$ or $[V(Np\text{-tolyl})(OEt)_3]$ affording $[VOCax(O)_3(OMe)(NCMe)]\cdot 2.5MeCN$ (**11**·2.5MeCN) and $[V(Np\text{-tolyl})Cax(O)_3(OMe)(NCMe)]$ (**12**), respectively. Both **11** and **12** are readily recrystallised from saturated solutions of acetonitrile on prolonged standing at ambient temperature to afford crystals, in good yields (60–70%), suitable for single crystal X-ray diffraction using synchrotron radiation.

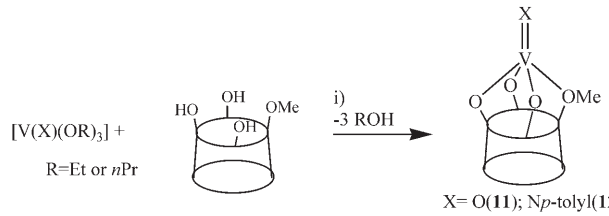

Scheme 6. Synthesis of the complexes **11** and **12**. i) Toluene, reflux, 12 h.

The structure of **11** is illustrated in Figure 11. The geometry at vanadium atom is best described as distorted trigonal-bipyramidal with the oxo group and two calixarene aryl oxide oxygen atoms equatorial. The vanadyl bond length (1.5897(17) Å) is typical, whilst the V–O(Me) bond length (2.3054(19) Å) is, as expected, longer than those to the calixarene aryloxide oxygen atoms ($V-O_{av}=1.805(2)$ Å). Interestingly, the vanadyl group is slightly tilted away from the O(2)/O(3) face, and this is doubtless responsible for the observed kink at O(4) ("external" V(1)-O(4)-C(34) 154.40(14)°). There is a solvent molecule (MeCN) in the calixarene cavity, which is tilted due to the close proximity of a *tert*-butyl group to a neighbouring calixarene. The remaining 1.5 MeCN are outside the calixarene cavity—the 0.5 MeCN is on a symmetry element and has the methyl group disordered

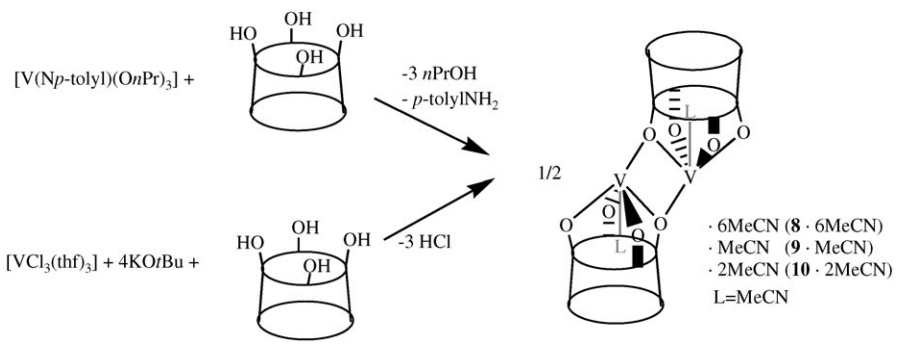

Scheme 5. Synthesis of the solvates **8**, **9** and **10**.

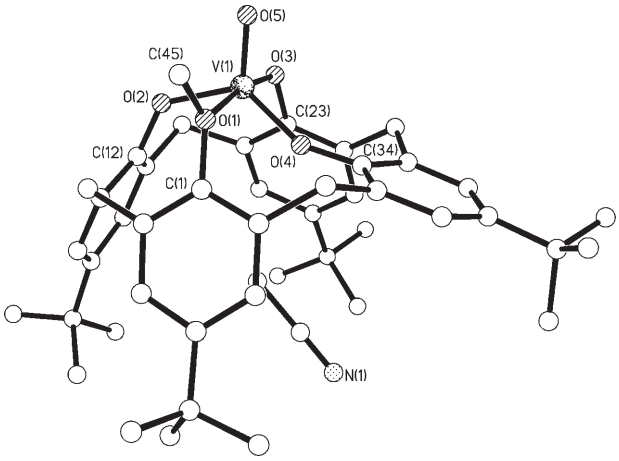

Figure 11. Molecular structure of **11**. Selected bond lengths [Å] and angles [°]: V(1)–O(1) 2.3054(19), V(1)–O(2) 1.8139(16), V(1)–O(3) 1.8260(18), V(1)–O(4) 1.7747(15), V(1)–O(5) 1.5897(17); V(1)-O(1)-C(1) 118.44(12), V(1)-O(2)-C(12) 129.54(12), V(1)-O(3)-C(23) 118.72(13), V(1)-O(4)-C(34) 154.40(14), V(1)-O(1)-C(45) 126.61(19), O(1)-V(1)-O(5) 86.47(9), O(4)-V(1)-O(5) 118.95(9).

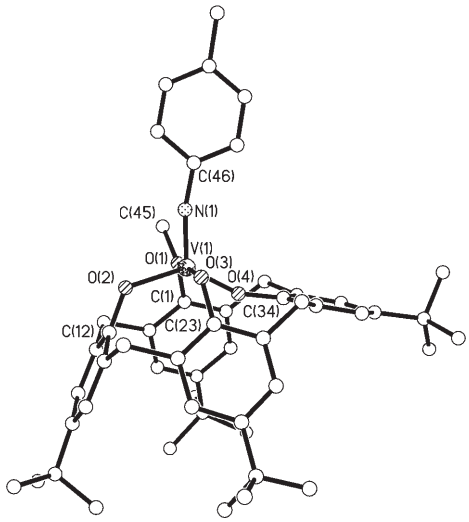

Figure 12. Molecular structure of one of the four molecules in **12**. Selected bond lengths [Å] and angles [°]: V(1)–O(1) 2.299(4), V(1)–O(2) 1.839(4), V(1)–O(3) 1.858(3), V(1)–O(4) 1.783(4), V(1)–N(1) 1.661(5), N(1)–C(46) 1.364(7); V(1)-O(1)-C(1) 117.3(3), V(1)-N(1)-C(46) 167.8(3).

over two sets of positions (50:50). The complex $[VOCax(O)_3(OMe)]$ has been previously prepared from the reaction of styrene oxide and $[\{VCax(O)_3(OMe)\}_2]$ and was structurally characterised as its diethyl ether/THF solvate with a similar conformation, but with the corresponding angles at O(2) and O(4) more linear (141.7 and 167.6°, respectively) than in **11**.[13] Related structures have also been observed by Limberg et al.,[13c] in which the cone and partial cone conformations are close in energy and the favoured conformation is reliant upon the crystallisation conditions employed.

We note that in a recent review, Radius has structurally characterised the *tert*-butylimido complex $[V(N\mathit{t}Bu)Cax(OMe)(O)_3]$ and that phenyl and *p*-tolylimido derivatives have been prepared by the interaction of the lithium salt $Cax(OMe)(OLi)_3$ and the respective trihalide, namely $[V(NAr)Cl_3]$ (Ar = Ph, *p*-tolyl).[18] We have also used this route to prepare the *p*-tolylimido analogue of **11**; however, we find that the same *p*-tolylimido compound **12** can be isolated in better yields upon interaction of the parent ligand $Cax(OMe)(OH)_3$ with $[V(N\text{-}p\text{tolyl})(OEt)_3]$. Single crystals suitable for a structure determination using synchrotron radiation can readily be grown form a saturated solution of acetonitrile on prolonged standing at ambient temperature.

The structure complex **12** is shown in Figure 12, with selected bond lengths and angles given in the caption. There are four molecules of the vanadium calixarene in the asymmetric unit, each of which are very similar (both geometry and conformation), and have an acetonitrile (not metal bound) residing in the bowl.

There is also a further acetonitrile, modelled at half-weight, giving an overall formula of $[V(N\text{-}p\text{-tolyl})Cax(OMe)(O)_3]\cdot 1.125\,MeCN$ (**12**·1.125 MeCN). In each molecule, the OMe group is disordered over two positions on opposite sides of the calixarene, and this is doubtless due to the close approach of two of the molecules and subsequent π-stacking of a calixarene face of one molecule with the ring of the *p*-tolylimido group of the other (and vice versa). The geometry at each vanadium atom, as in **11**, is best described as distorted trigonal bipyramidal, with one of the calixarene oxygen atoms (for example, O(1)/O(3)) occupying the axial positions. Similarly, again there is a kink at O(4) ("external" V(1)-O(4)-C(34) 157.5(3)°) as a result of the bending of the imido group from the O(2)/O(3) face. The V–O(-Ar) bonds fall in the range 1.769(3)–1.895(4) Å and are similar to those for the other compounds described herein and elsewhere,[19] whilst those to the OMe group are somewhat longer (2.281(3)–2.299(4) Å). The imido groups are short (V–N 1.649(4)–1.661(5) Å), and are best described as near linear (161.2(4)–170.6(4)°).

The bimetallic system, **13**, has been prepared by utilising the biscalix[4]arene ligand $[\{Cax(OH)_2(\mu\text{-}OpyO)\}_2]$[20] as depicted in Scheme 7.

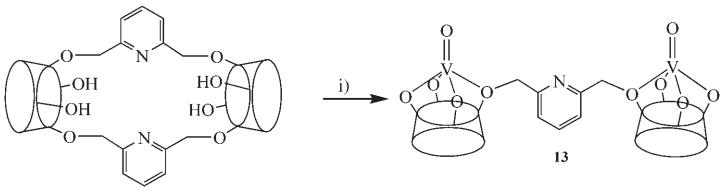

Scheme 7. Synthesis of the bridged complex **13**. i) $[VOCl_3]$, toluene, 12 h.

Reaction of the biscalix[4]arene with $[VOCl_3]$ in refluxing toluene leads to loss of a bridge in the form of 2,6-lutidene and formation of the bimetallic complex $[\{V(O)Cax(O)_4\}_2(\mu\text{-}2,6\text{-}CH_2pyCH_2)]\cdot 4\,MeCN$ (**13**·4 MeCN).

This complex can be readily recrystallised on prolonged standing at ambient temperatures from saturated solutions

of either dichloromethane or acetonitrile. The use of acetonitrile afforded crystals suitable for single-crystal X-ray diffraction using synchrotron radiation. The molecule is shown in Figure 13; bond lengths and angles are given in the caption.

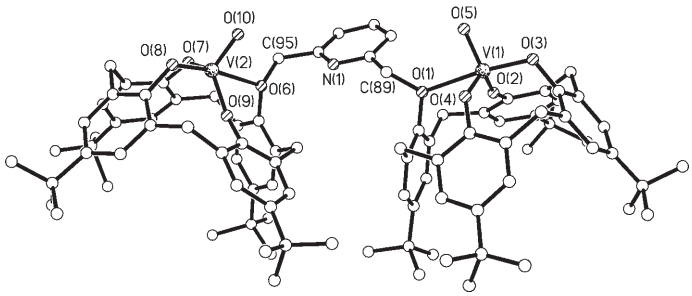

Figure 13. Molecular structure of **13**. Selected bond lengths [Å] and angles [°]: V(1)–O(1) 2.401(3), V(1)–O(2) 1.758(3), V(1)–O(3) 1.801(3), V(1)–O(4) 1.787(3), V(1)–O(5) 1.579(3), V(2)–O(10) 1.588(4); V(1)-O(1)-C(1), 117.1(2), V(1)-O(1)-C(89) 121.2(3), V(2)-O(6)-C(95), 121.2(3).

tion. In total, there are four acetonitrile molecules of crystallisation, three of which are well-defined. A molecule of acetonitrile is found in each of the calixarene cones, but is not bound to the vanadium atom. There is also a solvent molecule in the pocket created by the "lutidene" bridge and a phenoxide from each calix[4]arene. The remaining solvent molecule is external to the cavities and is split over two sites, each at 50% occupancy. Each vanadium atom adopts the trigonal bipyramidal geometry, for which both vanadyl groups are orientated in the same direction with respect to the lutidene bridge.

^{51}V NMR studies: The ^{51}V NMR shifts for the compounds reported herein, shown in Table 3, follow the trends previously noted. In particular, for related compounds such as **1** and **2** or **11** and **12**, imido shifts are more positive than oxo shifts; corresponding line widths are also larger for the imido species. Replacement of a *tert*-butoxide group with either a propoxide (as in **5** compared to **4**) or an aryloxide (as in **7** compared to [V(N*p*-tolyl)(O*t*Bu)$_3$]) also leads to a shift to more positive values. A plot of the inverse line width against the chemical shift for our compounds reveals two clusters, however, unlike in other studies,[21a,b] this plot is not helpful here in pre-determining the coordination number at vanadium, doubtless due to the more varied nature of the ligands employed herein.

Table 3. ^{51}V NMR shifts for **1**–**13** and related oxo and imido complexes.

Complex	δ [ppm]	$\omega_{1/2}$ [Hz]	Reference
1	−321.3	143	this work
2	−216.2	1998	this work
4	−586.6	134	this work
5	−545.6	144	this work
6	−592.9	865	this work
7	−352.8	353	this work
11	−354.6	907	this work
12	−322.6	925	this work
13	−371.5	2170	this work
[V(O)L^1]	−320	–	[4b]
[V(O)(O*t*Bu)$_3$]	−669	12	[11]
[V(O)(O*i*Pr)$_3$]	−624	13	[26b]
[V(N*p*-tolyl)(O*t*Bu)$_3$]	−654	–	[11]
[V(N*p*-tolyl)(O*i*Pr)$_3$]	−611	–	[26b]
[VO(OC$_6$H$_3$*i*Pr$_2$-2,6)$_3$]	−531.6	–	[21]
[VO(OC$_6$H$_3$Me$_2$)$_3$]	−511	20	[11]
[V(N*p*-tolyl)(OC$_6$H$_3$Me$_2$)$_3$]	−428	366	[11]

Polymerisation: We have screened a number of the compounds described herein as to their ability to polymerise ethylene (and ethylene/propylene co-polymerisation) in the presence of a number of organoaluminium co-catalysts, namely methylaluminoxane (MAO), dimethylaluminium chloride (DMAC) and trimethylaluminium (TMA) and with or without the re-activating substance ethyltrichloroacetate (ETA). In this context, we note that vanadyl aryloxides of the type [VO(OAr)$_3$] and [VCl(OAr)$_2$(THF)$_2$] (Ar = 2,6-*i*Pr$_2$C$_6$H$_3$) have been examined as pro-catalysts for ethylene polymerisation in the presence of a co-catalyst slurry of [MgCl$_2$(THF)$_2$] and [Et$_2$AlCl].[22] The associated activities of these systems however were unremarkable. There are also recent reports in the literature concerning the use of imido-vanadium aryloxide complexes as pro-catalysts for the homo- and co- and terpolymerisation of ethylene, ethylene/propene and ethylene/propene/diene,[6b,23] whilst we have previously screened [{V(N*p*-tolyl)}$_2$*p*-*tert*-butylcalix[8]areneH$_2$] in the presence of DMAC (no ETA) and observed an activity of 50 g mmol^{-1} h^{-1} bar^{-1}.[2f] The extremely active bi- and triphenolate pro-catalysts **IV** and **V** have also been screened under the conditions employed herein for comparative purposes.

As discussed elsewhere,[24] the role of ETA is thought to be that of a re-oxidising agent, whereby any inactive V^{II} species formed on reduction of the pro-catalyst by the excess DMAC are re-oxidised to re-enter the catalytic cycle as V^{III} or V^{IV} species; detrimental effects of ETA have also been previously noted.[6a] However, the exact role played by DMAC in obtaining such phenomenal activities is far from clear. Similarities between activities, molecular weights and polydispersity values for a number of these systems for polyethylene formation and ethylene/propylene co-polymerisation suggest related active species are formed, regardless of the ancillary ligand present. If this is indeed the case, then it is probable that the ancillary ligands are removed from the vanadium centre under the employed catalytic conditions. For systems based on acac-type ligands, for example **VI**, migration of ligands from V to Al has been noted, as confirmed by the isolation of [Al(acac)$_2$]$^+$.[25] In the case of phenoxide-type ligation, ligand abstraction by the aluminium co-catalyst is less pronounced, though a V^{2}Al$_4$ cluster (**VII**) has been isolated from [V(OAr)$_3$] (Ar = 2,6-*t*Bu$_2$C$_6$H$_3$) and EtAlCl$_2$, whilst the characterisation of species such as [Al(OAr)Me$_2$(THF)] suggests a disproportionation reaction is occurring. Gambarotta et al. have postulated that the

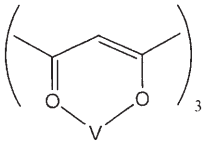

VI

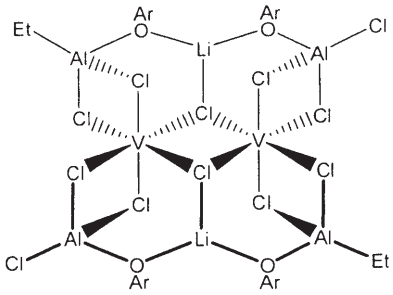

VII

Table 4. Bowl depths.[a]

Complex	Depth [Å]	Complex	Depth [Å]
1a	3.63	**6**	5.15 and 5.08
1b	3.14	**7**	5.10
2	3.69	**8**	4.91
3	2.99	**9**	4.63
4/5	5.00	**10/11**	4.75

[a] The bowl depth is defined as the distance between the centroid of the mean plane defined by the phenolate O atoms and the centroid of the mean plane defined by the central C atom of the *tert*-butyl group. [b] Complexes **12** and **13** have been omitted as these are not standard bowls.

active species is a large cluster in which ligands (phenoxide, halide and alkyl groups) are shared between both V and Al centres.[24]

In our systems, despite the apparent complex nature of the EPR spectra, the unimodal molecular weight distributions are consistent with the formation of single catalytically active species, both when DMAC and MAO are employed as co-catalysts in the presence of ETA. Nomura has suggested for his systems, based on $[VCl_2(N\text{-}2,6\text{-}Me_2C_6H_3)(OAr)]$ ($Ar = 2,6\text{-}Me_2C_6H_3$, 2,6-*i*$Pr_2C_6H_3$, 2,6-$Ph_2C_6H_3$), that the differing observed activities when employing DEAC (diethylaluminium chloride) or MAO as co-catalysts are the result of ion-pair effects.[8h] In the case of DEAC, the cationic vanadium alkyl formed is stabilised by an equilibrium involving a chloro-bridged (V-Cl-Al) species, whereas for MAO a discrete ion-pair is proposed. In our case, the situation is complicated by the chelating nature of the ancillary ligands and whether one or all bonds are broken between the vanadium and the calixarene under the conditions employed here. Although the nature of the active species formed upon addition of excess DMAC remains uncertain, the results presented herein suggest clear differences in catalytic performance when oxa(-CH_2OCH_2-)- or methylene(-CH_2-)-bridged calixarenes are employed as ancillary ligands in α-olefin polymerisation systems. The reasons for such differences in performance are thought to be both steric and electronic in nature and relate to the ease with which the macrocycle can be disconnected from the vanadium centre. The crystal structures of **1**–**13** reveal how the shape and size of the oxacalix[3]arene ligand (and associated cavity) is very different to that of the calix[4]arene ligand and this is clearly reflected in how these ligands bind to groups such as the vanadyl group, that is *exo* versus *endo*. For the oxacalixarene complexes, the vanadyl (or imido) group is *endo* (in the cavity) and as depicted in the crystal structures (Figure 2 and Figure 4), this renders the vanadium somewhat exposed. By contrast, for the calix[4]arenes, the vanadyl (or imido) group is *exo*. The depths of each type of cavity are also very different (see Table 4), with the bowl depth of the calix[4]arene in our pro-catalysts being typically about 5 Å (slightly less if there is an MeCN in the cavity), which is somewhat deeper than found for the oxacalix[3]arene pro-catalysts **1** (a 3.63 Å, b 3.14 Å) and **2** (3.69 Å). We note that vanadyl groups supported by flat phthalocyanine or porphyrin ligands afford low activity catalysts with either MAO or $EtAlCl_2$ as co-catalyst; reactivators were not used in this study.[26]

In the case of **5** and **13**, the observed high activities (cf **8**, **11** and **12**) may be the result of cooperative effects between the vanadium centres upon formation of the active species. In this respect, we note that 2–3x activity increases have been observed in imine systems of nickel upon coordination of a second metal.[27] For **5**, the two vanadyl centres are close (ca. 3.319 Å), whereas the situation in **13** would require considerable disruption of the pro-catalyst structure, which is clearly feasible given the large excesses of co-catalyst employed herein.

Oxacalix[3]arene complexes 1 and 2: We have examined herein the catalytic behaviour of **1** and **2** with and without ETA present to observe if this would be of benefit to the performance (activity) of these systems. For both **1a,b** and **2**, dramatic changes/increases in activity and catalyst lifetime were observed in the presence of ETA. In particular, the behaviour of these systems under elevated temperatures (conditions more suited to industrial use), showed the most interesting changes. Both **1** and **2** showed an upward trend in activity with increasing temperature, and activities as high as 130000 $g\,mmol^{-1}\,h^{-1}\,bar^{-1}$ (15-minute runs) were readily achievable at 80 °C. At such elevated temperatures, high activities are also possible for much smaller co-catalyst loadings, for example at 80 °C, activities in excess of 40000 $g\,mmol^{-1}\,h^{-1}\,bar^{-1}$ are achievable using an [Al]:[V] ratio of 800:1. The use of less than 200 equivalents of DMAC affords negligible polymer, which is doubtless a reflection of the need for a minimum amount of co-catalyst required to carry out scavenging duties.

The temperature increase leads to a dramatic decrease in polymer molecular weight—at 25 °C, ultra-high-molecular-weight (>5500000) polymer is formed, which falls to less than 500000 at 80 °C. At 7 bar in an autoclave, both **1** and **2** afforded solid polyethylene with an activity of about 900000 $g\,mmol^{-1}\,h^{-1}$ (or ~130000 $g\,mmol^{-1}\,h^{-1}\,bar^{-1}$). For comparison, we have also re-tested the bi- and triphenolate complexes **IV** and **V** under these more robust catalytic conditions (see Table 5). Both **IV** and **V** show impressive activities (ca. 157,000 $g\,mmol^{-1}\,h^{-1}\,bar^{-1}$) at 80 °C, yielding polymers with molecular weights of 346000 and 383000, respec-

Table 5. Ethylene polymerisation results[a] for **1** and **2**.

Catalyst	Temperature [°C]	Yield [g]	Activity [g mmol^{-1}(**V**) h^{-1} bar^{-1}]	[η] [dL g^{-1}]	M_w	M_n	M_w/M_n	P.E. m.p. [°C]
1	25	1.27	25300	19.1	5510000	1620000	3.4	133.3
1	80	4.63	92500	3.45	463000	232000	2.0	133.0
2	25	0.67	13400	24.2	6160000	1860000	3.3	135.5
2	80	6.47	129400	3.15	421000	191000	2.0	133.9
IV	25	1.87	37400	13.2	–	–	–	
IV	80	7.86	157200	2.90	346000	164000	2.1	
V	25	2.31	46100	15.6	–	–	–	
V	80	7.83	15600	3.13	383000	173000	2.2	

[a] All runs completed in the presence of pro-catalysts (0.0008 mmol L^{-1}), DMAC (2 mmol L^{-1}), ETA (2 mmol L^{-1}) in toluene (250 mL) over a period of 15 min. Reactions quenched with dilute HCl, washed with methanol (50 mL) and dried for 12 h in a vacuum oven at 45 °C.

tively. For **1a,b** and **2**, the co-catalyst used is crucial, for example with methylaluminoxane (MAO) the catalysts are best described as poor to moderate (<50 g mmol^{-1} h^{-1} bar^{-1}). When using DMAC, the activity of the system is a function of the [Al]/[V] concentration ratio and increases in an almost linear fashion. Such a linear dependence is suggestive of non-innocent behaviour for DMAC. In the absence of ETA, activities are far lower (≤ 10000 g mmol^{-1} h^{-1} bar^{-1}), and vary with temperature such that there is an increase until about 45 °C for **1a** and 30 °C for **2**, whereupon there is a decrease, and this is most likely a result of catalyst instability.

For all runs, melting points (by DSC) are around 135 °C, typical of linear polyethylene. In no case has polyethylene been obtained using **1a,b** or **2** in the absence of aluminium co-catalyst, whilst the use of up to 7000 equivalents of DMAC under the conditions employed here afforded negligible polymer.

Pro-catalysts **1** and **2** (and **IV** and **V**) have also been screened for ethylene/propylene copolymerisation; results are presented in Table 6. The activity observed for **1** (9700 g mmol^{-1} h^{-1} bar^{-1}) is somewhat higher than that observed for **2** (3900 g mmol^{-1} h^{-1} bar^{-1}) with similar (14.6 and 14.5 mol %) propylene incorporation. Pro-catalysts **IV** and **V** are more active (16500 and 19300 g mmol^{-1} h^{-1} bar^{-1}, respectively), and again have similar (14.5 and 15.4 mol %) propylene incorporation.

Calix[4]arene complexes: To determine whether the dimethyloxa(-CH_2OCH_2-) bridge of the oxacalixarene was a prerequisite for the high activities observed in our calixarene-based systems, we also screened the methylene(-CH_2-)-bridged calix[4]arene complexes **5**, **8**, **11, 12** and the bridged bis-calix[4]arene complex **13** in the presence of a number of organoaluminium co-catalysts and ETA.

The pro-catalysts **5**, **8**, **11**, **12** and **13**, in the presence of DMAC and ETA, showed very good activity with respect to the Gibson criteria for the polymerisation of ethylene (Figure 14).[28a] In particular, the activities resulting from the use

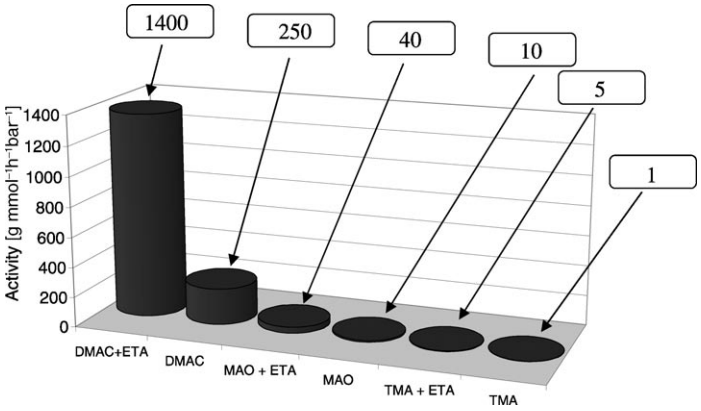

Figure 14. Activity versus co-catalysts variation for pro-catalyst **11**.

Table 6. Ethylene/propylene copolymerisation results[a] for **1** and **2** at 25 °C.

Catalyst	Yield [g]	Activity [g mmol^{-1} h^{-1} bar^{-1}]	[η] [dL g^{-1}]	M_w	M_n	M_w/M_n	C_3 = content [mol %]
1	0.485	9700	8.76	2980000	1370000	2.2	14.6
2	0.196	3900	9.36	3520000	1790000	1.9	14.5
IV	0.825	16500	10.1	1240000	464000	2.6	14.5
V	0.963	19300	10.4	1390000	504000	2.8	15.4

[a] Runs completed in the presence of pro-catalysts (0.0008 mmol L^{-1}), DMAC (2 mmol L^{-1}), ETA (2 mmol L^{-1}) in toluene (250 mL) over a period of 15 min, 50:50 feed ethylene:propylene. Reactions quenched with dilute HCl, washed with methanol (50 mL) and dried for 12 h in a vacuum oven at 45 °C.

of **5** and **13** were around an order of magnitude greater than those observed for **8**, **11** and **12**.

The polyethylene produced (see Table 7) using **5** and **13** had molecular weight in the range 89000–113000, whilst that generated by using **8**, **11** and **12** exhibited somewhat higher molecular weights (177000–ca. 433000); all with narrow molecular weight distributions (2.1–2.5) and melting points ca. 135 °C, typical for linear polyethylene. As for the oxacalix[3]arene system, a study of co-catalyst concentration (DMAC) yielded a direct linear [Al]/[V] relationship. The activity of the calix[4]arene systems was found to peak at

Table 7. Ethylene polymerisation results.

Pro-catalyst	Co-catalyst equivalents	Activity[a]	M_w	M_n	M_w/M_n	P.E. T_m [°C]
5	4000	8700	89600	39700	2.3	135
8	4000	1300	182000	81725	2.3	135
11	4000	1400	433250	205000	2.1	134
12	4000	1500	177000	86150	2.1	136
13	10000	10400	113000	45200	2.5	135

[a] ($g\,mmol^{-1}$(**V**)$\,h^{-1}\,bar^{-1}$). All runs completed in the presence of ETA (0.1 mL) and 1.0 M DMAC over a period of 60 min. Reactions quenched with dilute HCl, washed with methanol (50 mL) and dried for 12 h in a vacuum oven at 45 °C. Schlenk line reaction in toluene (100 mL).

45 °C. The activities observed for the best of the methylene bridged calix[4]arene complexes, **5** and **13**, are however, still of an order of magnitude lower than those observed for the oxacalix[3]arene systems and interestingly also than those observed for the -CH_2- bridged bi- and triphenolates **IV** and **V**.

The dimeric vanadium(IV) complex [{VCax$(O)_4$-(NCMe)}$_2$]·6MeCN (**8**·6MeCN) displays properties similar to those exhibited by the monomeric complexes **11** and **12** (e.g. $M_w = 182000$; $M_w/M_n = 2.3$; 1300 $g\,mmol^{-1}\,h^{-1}\,bar^{-1}$ for **8** compared with $M_w = 177000$; $M_w/M_n = 2.1$; 1500 $g\,mmol^{-1}\,h^{-1}\,bar^{-1}$ for **12**), and the catalyst lifetimes follow similar profiles.

The activity trends observed for the variation of co-catalyst for the calix[4]arene complexes follow the same trend as observed when employing either **1** or **2** as pro-catalyst. For all runs, the absence of ETA has a detrimental effect upon activity, for example, for **11**/DMAC: 1400 to 250 $g\,mmol^{-1}\,h^{-1}\,bar^{-1}$ (see Figure 14), and for **11**/MAO 40 to 10 $g\,mmol^{-1}\,h^{-1}\,bar^{-1}$.

EPR studies: Previous EPR studies on vanadium-based Ziegler-type catalysts suggest that these systems are rather complex, forming multiple species. For example, the [Cp_2VCl_2]/$EtAlCl_2$ system formed at least three EPR active species, one of which was identified as [$Cp_2VCl(\mu\text{-}Cl)_2AlCl_2$];[29a] later the hydride [$Cp_2VH(\mu\text{-}Cl)_2AlCl_2$] was also proposed.[29b]

For **1**, quantitative studies against a standard [$VO(acac)_2$], of known concentration [1 mmol] have been carried out. Comparison with the standard suggests there is an appreciable amount of V^{IV} formed on addition of excess DMAC to **1**. For 10 equivalents of DMAC, when ETA is absent, the initial concentration of V^{IV} is about 60%, which falls to about 24% after 1 h. The frozen glass spectrum of **1**, at this concentration of DMAC (no ETA), at $t = 60$ min is characteristic of a vanadium(IV) species and consists of an anisotropic signal with eight-line hyperfine structure ($g_{x,y} = 1.99/1.99$, A_{xy} 70/70; $g_z = 1.97$, A_z 177). In the presence of ETA the initial concentration of V^{IV} is about 26%, which falls to about 16% over 1 h. Interestingly, similar experiments for 500 equivalents of DMAC, in the absence of ETA, show that the V^{IV} concentration remains fairly constant at 55–60% over 1 h, whilst in the presence of ETA, there is an initial high concentration of V^{IV} (80–85%) which falls to about 70% over 1 h. At these higher concentrations, with and without ETA, there is also a signal in the half-field region ($g = 4$), the strength of which is suggestive of aggregation rather than simple dimer formation. It was not possible to increase the [V]:[Al] ratio beyond 1:500 without severe deterioration in the quality of the spectra. The inaccuracy usually associated with concentration experiments of this type (±20%) should also be noted.

Conclusion

We have prepared and structurally characterised a series of new *p-tert*-butylhexahomotrioxacalix[3]arene and *p-tert*-butylcalix[4]arene complexes bearing vanadyl or imidovanadium groups, and have examined their catalytic activity for ethylene polymerisation and copolymerisation with propylene. The crystal structure analyses reveal rare examples of monomeric *p-tert*-butylhexahomotrioxacalix[3]arene metal complexes (**1** and **2**), together with complexes (**4** and **5**) in which two metal centres are bound to just one calix[4]arene ligand, a novel example (**6**) of an Li_4O_4 cube 'sandwiched' between two calix[4]arene ligands, and a complex (**13**) in which two metallocalix[4]arene fragments are linked through a lutidene bridge. Among them, **1** and **2**/DMAC/ETA displayed the highest activity for ethylene polymerisation (up to 130000 $g\,mmol^{-1}\,h^{-1}\,bar^{-1}$ at 80 °C, yielding ultra-high-molecular-weight (>5500000), linear polyethylene), and ethylene/propylene copolymerisation (up to 10000 $g\,mmol^{-1}\,h^{-1}\,bar^{-1}$ at 25 °C) with about 14.5 mol% propylene incorporation. These activities are amongst the highest reported to-date for non-metallocene systems,[28] and both **1** and **2** are stable to prolonged exposure to air. The use of other organoaluminium co-catalysts such as MAO leads to much poorer catalytic activities. Calix[4]arene-based pro-catalysts are at best an order of magnitude less active than those observed for **1** and **2**; those containing two vanadium centres (**5** and **13**) exhibit the highest activity for this class. The exact role played by DMAC is still far from clear, however, we are now focussing on the identification of the active species in these vanadium-based systems. This will be a major step forward in our understanding, and will provide information vital to the future design of new vanadium-based catalytic systems.[34]

Experimental Section

General: All manipulations were carried out under an atmosphere of nitrogen using standard Schlenk and cannula techniques or in a conventional nitrogen-filled glove-box. Solvents were refluxed over an appropri-

ate drying agent, and distilled and degassed prior to use. Elemental analyses were performed by the microanalytical services of the School of Chemical Sciences and Pharmacy at The University of East Anglia or Medac Ltd. NMR spectra were recorded on a Varian VXR 400 S spectrometer at 400 MHz or a Gemini at 300 MHz (^{1}H), 75.5 MHz (^{13}C) and 105.1 MHz (^{51}V) at 298 K; chemical shifts are referenced to the residual protio impurity of the deuterated solvent. EPR spectroscopy was performed on an X-band ER200-D spectrometer (Bruker Spectrospin) interfaced to an ESP1600 computer and fitted with a liquid helium flow cryostat (ESR-900; Oxford Instruments). EPR spectra were simulated with Simfonia. IR spectra (nujol mulls, KBr/CsI windows) were recorded on Perkin-Elmer 577 and 457 grating spectrophotometers. The precursors [V(N*p*-tolyl)Cl$_3$], [V(N*p*-tolyl)(O*t*Bu)$_3$], [V(N*p*-tolyl)(O*n*Pr)$_3$], [V(N*p*-tolyl)(OEt)$_3$] and [VCl$_3$(THF)$_3$] were made by the methods of Maatta, van Koten and Kurras.[11,30,31] The ligands Cax(OH)$_4$, Cax(OH)$_2$(OMe)$_2$ and Cax(OH)$_3$(OMe) were prepared by the previously published procedures.[32] All other chemicals were obtained commercially and used as received unless stated otherwise.

Ethylene polymerisation procedure: Ethylene polymerisations were performed in a flame-dried glass flask (250 mL) equipped with a magnetic stirrer bar. The flask was evacuated and filled with ethylene gas at 1 bar pressure, which was maintained throughout the polymerisation. The flask was further purged several times with ethylene and then dry and degassed toluene (100 mL) was added by using a dry glass syringe. The reactivating agent ETA was added (0.1 mL, 0.72 mmol) if applicable, and the solution was stirred for 10 min, allowing ethylene saturation and the correct temperature to be acquired by the use of a water bath. After saturation, the co-catalyst was added (DMAC, between 50–10000 equivalents [Al]/[V] with respect to the vanadium pro-catalyst). The pro-catalyst was injected as a toluene solution (a stock solution of 0.1–3.125 μmol per mL of pro-catalyst in toluene was prepared and pro-catalyst loadings of 0.1–3.125 μmol were employed, depending on the activity of the pro-catalyst). The polymerisation time was taken from pro-catalyst injection, lasting for 15 min–1 h. The polymerisation was quenched upon the injection of methanol (5 mL). The resultant polymer solution was transferred into a 500-mL beaker containing acidified methanol and the solid polyethylene was collected by filtration and dried in vacuo at 90 °C overnight, unless otherwise stated.

Autoclave procedure: A 1-L Büchiglasuster steel autoclave was used for high-pressure testing of pro-catalysts **1**–**6**. A Büchi pressflow pressure regulator was used to control the systems pressure, and the temperature was regulated by a Julabo FP50 heater-chiller device. The flask was evacuated overnight at 120 °C, after ensuring that the system was air tight at 7 bar of ethylene or argon pressure. The flask was flushed with ethylene several times then, after the temperature had been set to 80 °C, 400 mL of dry toluene (containing 15 mL, 15 mmol, of 1 M DMAC and 1 mL, 7.2 mmol, of ETA) was transferred by cannula into the flask. The system was stirred vigorously with a mechanical stirrer until the polymerisation was terminated. The pro-catalyst was injected (0.1 μmol as a 5 mL stock solution in toluene through a pressurised valve) after the toluene solution was saturated with ethylene (gas consumption dropped to a negligible amount) by purging several times with ethylene. The system was kept at an ethylene pressure of 7 bar throughout the polymerisation, and the time was taken from pro-catalyst injection to polymerisation termination (by injecting 5 mL methanol) which was 1 hour. The pressure was released and the solid polyethylene was quenched in an acidic methanol solution. The polymer was collected by filtration and dried overnight in vacuo at 90 °C.

Complex syntheses

Complex [V(O)L] (1): Hexahomooxacalix[3]areneH$_3$ (LH$_3$) (1.00 g, 1.73 mmol) and [V(O)(O*n*Pr)$_3$] (0.40 mL, 1.78 mmol) in toluene (40 mL) were warmed to 60 °C for 2 h. (Longer reaction times lead to the formation of green reduced species). Following removal of volatiles in vacuo, the solid residue was extracted into warm acetonitrile (2×30 mL). Prolonged standing (1–2 days) at ambient temperature afforded golden-yellow crystals of **1** (0.39 g, 35 % yield).

Alternative synthesis of **1**: Hexahomooxacalix[3]areneH$_3$ (1.00 g, 1.73 mmol) and [V(mesityl)$_3$THF] (0.83 g, 1.73 mmol) were combined in THF (40 mL) at −78 °C. The mixture was allowed to warm to ambient temperature and was stirred for 2 h. Dry oxygen was bubbled through the system for 5 min, after which volatiles were removed in vacuo and the residue was extracted into warm acetonitrile (40 mL). Prolonged standing at ambient temperature afforded large prisms of **1**, 0.42 g, 38 % yield. Elemental analysis calcd (%) for $C_{36}H_{43}O_7V{\cdot}CH_3CN$: C 67.1, H 6.8, N 2.0; found: C 66.9, H 7.0, N 1.9; m.p. >350 °C; ^{1}H NMR (CDCl$_3$): δ = 7.30 (s, 6H; Ar-*H*), 4.83 (d, $^2J_{H,H}$ = 9.1 Hz, 6H; OCH$_2$), 4.50 (d, $^2J_{H,H}$ = 9.1 Hz, 6H; OC*H*$_2$), 1.92 (s, 3H; MeCN), 1.27 ppm (s, 27H; C(C*H*$_3$)$_3$); ^{13}C NMR (CDCl$_3$): δ = 166.76, 144.87, 126.30, 122.91, 71.41, 33.30, 30.49 ppm; ^{51}V NMR (CDCl$_3$): δ = −321.3 ($\omega_{1/2}$ 143 Hz); IR (cm^{-1}): $\tilde{\nu}$ = 1301w, 1260m, 1194s, 1117m, 1081s, 1035s, 1015s, 969m, 928w, 876m, 841m, 789s, 717m, 666w, 625w, 585m; MS (E.S.): *m*/*z*: 641 [*M*+H]$^+$, 658 [*M*+NH$_4$]$^+$, 663 [*M*+Na]$^+$.

Complex [V(N*p*-tolyl)L]$_2$ (2): As for **1**, but using [V(N*p*-tolyl)(OEt)$_3$] (0.56 g, 1.91 mmol) and (LH$_3$) (1.11 g, 1.92 mmol) afforded **2** as golden-yellow crystals (1.14 g, 45 % yield). Elemental analysis calcd (%) for $C_{86}H_{104}N_2O_{12}V_2$: C 70.8, H 7.1, N 1.9; found: C 70.7, H 7.2, N 2.0; m.p. >350 °C (decomposed at ca. 300 °C). ^{1}H NMR (CDCl$_3$): δ = 7.21 (overlapping singlets, 12H; Ar-*H*), 6.18 (d, $^3J_{H,H}$ = 8.3 Hz, 4H; tolyl-*H*), 5.51 (d, $^3J_{H,H}$ = 8.3 Hz, 4H; tolyl-*H*), 5.14 (d, $^2J_{H,H}$ = 8.8 Hz, 12H; OCH$_2$), 4.38 (d, $^2J_{H,H}$ = 8.8 Hz, 12H; OCH$_2$), 1.93 (s, 6H; *p*-tolyl-C*H*$_3$), 1.16 ppm (s, 54H; C(C*H*$_3$)$_3$); ^{13}C NMR (CDCl$_3$): δ = 167.42, 144.86, 142.79, 135.57, 126.44, 126.38, 126.30, 126.21, 124.78, 122.94, 71.58, 71.42, 33.30, 30.56, 20.17 ppm; ^{51}V NMR (CDCl$_3$): δ = −216.2 ppm ($\omega_{1/2}$ 1998 Hz); IR (cm^{-1}): $\tilde{\nu}$ = 1588w, 1362s, 1352m, 1306m, 1260s, 1214s, 1199s, 1168w, 1122m, 1081s, 1019m, 994w, 963w, 881 m, 840m, 809m, 789s, 758w, 718m, 671m, 620w, 604w, 574s; MS (E.S.): *m*/*z*: 1460 [*M*+H]$^+$, 1477 [*M*+NH$_4$]$^+$, 1482 [*M*+Na]$^+$.

Complex LH$_3$·MeCN (3): A solution of 2,6-bis(hydroxymethyl)-4-*tert*-butylphenol (30 g, 0.14 mol) in xylene (140 mL) was refluxed (with Dean–Stark) for 15 h. Best yields were obtained by allowing the mixture to stand at 80–90 °C for 1 h and then heating under gentle reflux for 2–3 h at 130 °C and finally heating under reflux for 15 h. On cooling, volatiles were removed by using a rotary evaporator. To the residue, hot hexane (150 mL) was added, the precipitate was filtered to afford colourless solid LH$_3$ (7.50 g, 27 %). A portion of this solid was then dissolved in hot MeCN and on cooling to ambient temperature colourless prisms of **3** slowly formed. M.p. 220–222 °C; ^{1}H NMR (CDCl$_3$): δ = 8.57 (s, 3H; OH), 7.12 (s, 6H; Ar-*H*), 4.72 (s, 12H; CH$_2$O), 1.24 (s, 27H; C(CH$_3$)$_3$), 1.19 ppm (s, 3H; MeCN); ^{13}C NMR (CDCl$_3$): δ = 153.63, 142.43, 126.92, 123.78, 100.26, 71.69, 33.87, 31.40 ppm; IR (cm^{-1}): $\tilde{\nu}$ = 3583w, 3376bm, 3329bm, 2924bs, 2293w, 2252m, 1654w, 1609m, 1487s, 1392m, 1304m, 1264m, 1209s, 1122m, 1077s, 1009 m, 972m, 900w, 879 m, 823w, 764w, 722m, 666m. Drying of the sample in vacuo removed the solvent (MeCN) of crystallisation.

[{VO(O*t*Bu)}$_2$(μ-O)Cax(OMe)$_2$(O)$_2$]·2MeCN (4·2MeCN): [V(O)(O*t*Bu)$_3$] (1.0 g, 3.49 mmol) and calix[4]arene(OH)$_2$(OMe)$_2$ (2.30 g, 3.40 mmol) were refluxed in toluene (30 mL) for 12 h. Following removal of volatiles in vacuo, the residue was dissolved in hot MeCN (30 mL), filtered and left to stand (1–2 days) at ambient temperature to afford **4** as red-brown prisms (958 mg, 30 % yield). Elemental analysis calcd (%) for $C_{54}H_{76}O_9V_2{\cdot}2CH_3CN$: C 66.1, H 7.9, N 2.7; found: C 65.7, H 8.3, N 2.6; m.p. 163 °C (decomp); ^{1}H NMR (CDCl$_3$): δ 7.25 (s, 4H; Ar-*H*), 6.90 (s, 4H; Ar-*H*), 4.48 (d, $^2J_{H,H}$ = 12.7 Hz, 4H; *endo*-CH$_2$), 4.13 (s, 3H; OCH$_3$), 3.49 (s, 3H; OCH$_3$), 3.35 (d, $^2J_{H,H}$ = 12.7 Hz, 4H; *exo*-C*H*$_2$), 1.46–1.36 (overlaying singlets, 36H; C(CH$_3$)$_3$), 1.02 (s, 9H; OC(CH$_3$)$_3$), 0.88 ppm (s, 9H; OC(CH$_3$)$_3$); ^{13}C NMR (CDCl$_3$): δ = 152.10, 151.72, 145.83, 145.45, 125.57, 125.37, 123.34, 123.25, 63.30, 62.64, 31.63, 34.19, 33.61, 30.87 ppm; ^{51}V NMR (C$_6$D$_6$): δ = −586.6 ppm ($\omega_{1/2}$ 134 Hz); IR (cm^{-1}): $\tilde{\nu}$ = 3324bw, 3234w, 3052w, 2962m, 2900m, 2867m, 2819w, 2388w, 2276s, 1617s, 1480m, 1455m, 1435w, 1393w, 1363 m, 1330m, 1300w, 1259m, 1207m, 1161m, 1122m, 1065m, 1012m, 996m, 949m, 920w, 871 m, 859m, 800s, 774m, 742w, 665w; MS (ES): *m*/*z*: 976 [*M*].

[{VO(O*n*Pr)}$_2$(μ-O)Cax(OMe)$_2$(O)$_2$]·1.5MeCN (5·1.5MeCN): [V(O)(O*n*Pr)$_3$] (0.80 mL, 3.52 mmol) and calix[4]arene(OH)$_2$(OMe)$_2$ (2.30 g, 3.40 mmol) were refluxed in toluene (30 mL) for 12 h. Following removal of volatiles in vacuo, the residue was dissolved in hot MeCN (30 mL), fil-

tered and left to stand (1–2 days) at ambient temperature to afford **5** as red-brown prisms (787 mg, 25% yield). Elemental analysis calcd (%) for $C_{73}H_{96}O_9V_2\cdot CH_3CN$: C 71.3, H 8.1, N 1.1; found: C 71.6, H 8.2, N 1.4; m.p. 171°C (decomp); ^{1}H NMR ($CDCl_3$): δ = 7.68–6.75 (several m, 8H; Ar-*H*), 5.45–5.61 (m, 4H; OCH_2), 4.46 (d, $^2J_{H,H}$ = 12.8 Hz, 4H; *endo*-CH_2), 4.13 (s, 6H; OCH_3), 3.53 (d, $^2J_{H,H}$ = 12.8 Hz, 4H; *exo*-CH_2), 2.05 (m, $^3J_{H,H}$ = 6.9 Hz, 4H; CH_2CH_3), 1.51 (s, 18H; $C(CH_3)_3$), 1.45 (s, 18H; $C(CH_3)_3$), 1.2 (s, 21H; 7×MeCN), 1.03 ppm (m, 6H; CH_2CH_3); ^{13}C NMR ($CDCl_3$): δ = 152.00, 146.00, 145.56, 125.67, 125.52, 123.21, 63.19, 63.05, 34.24, 33.56, 31.49, 26.64, 10.30 ppm; ^{51}V NMR (C_6D_6): δ = −545.5 ppm ($\omega_{1/2}$ 144 Hz); IR (cm^{-1}): $\tilde{\nu}$ = 3331bw, 2249w, 1598w, 1482s, 1463s, 1393w, 1362m, 1300m, 1259m, 1206s, 1124w, 1094m, 1062w, 1014s, 994s, 942w, 917w, 871w, 800s, 721w, 665m; MS (E.S.): *m*/*z*: 942 [*M*]$^+$, 927 [*M*−CH_3].

[{VO(O*t*Bu)Cax(OMe)$_2$(O)$_2$}$_2$Li$_4$O$_2$]·8MeCN (6·8MeCN): [$VOCl_3$] (1.0 mL, 10.62 mmol) and LiO*t*Bu (2.72 g, 33.98 mmol) were combined in diethyl ether (40 mL) at −78°C, allowed to warm to room temperature and stirred for 3 h. Following removal of volatiles in vacuo, $(Me_3Si)_2O$ (1.13 mL, 5.32 mmol) in dichloromethane (40 mL) was added and stirring was continued for 6 h. Volatiles were again removed in vacuo, and calix[4]arene$(OH)_2(OMe)_2$ (3.59 g, 5.31 mmol) in toluene (40 mL) was added and the system was refluxed for 6 h. On cooling, volatiles were removed and the residue was extracted into warm MeCN (40 mL) to afford **6** as yellow needles (5.03 g, 55% yield). Further crops of **6** can be obtained from the mother-liquor (7.12 g, 78% total yield). Elemental analysis calcd (%) for $C_{100}H_{134}Li_4O_{14}V_2$: C 71.6, H 8.0; found: C 70.5, H 7.7; m.p. 185°C (decomp); ^{1}H NMR ($CDCl_3$): δ = 7.20–6.86 (bm, 16H; Ar-*H*), 4.60 (d, $^2J_{H,H}$ = 13.5 Hz, 4H; *endo*-CH_2), 4.18 (d, $^2J_{H,H}$ = 13.0 Hz, 4H; *endo*-CH_2), 3.39 (d, $^2J_{H,H}$ = 13.5 Hz, 4H; *exo*-CH_2), 3.29 (s, 6H; $ArOCH_3$), 3.28 (d, $^2J_{H,H}$ = 13.0 Hz, 4H; *exo*-CH_2), 3.12 (m, 6H; $ArOCH_3$), 1.91 (s, 3H; CH_3CN), 1.26–1.17 (overlaying singlets, 54H; $C(CH_3)_3$), 1.00 (s, 18H; $C(CH_3)_3$), 0.79 (s, 9H; $VOC(CH_3)_3$), 0.74 ppm (s, 9H; $VOC(CH_3)_3$); ^{13}C NMR ($CDCl_3$): δ = 151.34, 150.63, 146.96, 128.01, 125.63, 63.47, 63.06, 33.82, 33.46, 31.64, 30.92 ppm; ^{51}V NMR (C_6D_6): δ = −200 ppm ($\omega_{1/2}$ ~18 KHz); IR (cm^{-1}): $\tilde{\nu}$ = 3337bw, 2283w, 2248w, 1599 m, 1481 s, 1457 s, 1392w, 1376s, 1361s, 1300w, 1206s, 1169s, 1091s, 1015s, 985w, 892w, 850w, 799s, 705w, 665w.

[V(N*p*-tolyl)(O*t*Bu)$_2$Cax(OMe)$_2$(O)(OH)]·5MeCN (7·5MeCN): [V(N*p*-tolyl)(O*t*Bu)$_3$] (1.0 g, 2.66 mmol) and calix[4]arene$(OH)_2(OMe)_2$ (1.79 g, 2.64 mmol) were refluxed in toluene (30 mL) over activated 4 Å molecular sieves for 6 h. Volatiles were removed in vacuo, and the residue was extracted into hot MeCN (40 mL), cooling to ambient temperature afforded yellow-orange prisms of **7** (0.52 g, 20% yield). Elemental analysis calcd (%) for $C_{61}H_{84}NO_6V\cdot CH_3CN$: C 74.2, H 8.6, N 2.8; found: C 74.2, H 8.3, N 3.0. M.p. 182°C (decomp). ^{1}H NMR ($CDCl_3$): δ = 7.26 (s, 4H; Ar-*H*), 7.19 (d, $^3J_{H,H}$ = 8.3 Hz, 2H; tolyl-*H*), 6.94 (s, 4H; Ar-*H*), 6.86 (d, $^3J_{H,H}$ = 8.3 Hz, 2H; tolyl-*H*), 4.43 (d, $^2J_{H,H}$ = 13.1 Hz, 4H; *endo*-CH_2), 3.42 (s, 6H; OCH_3), 3.32 (d, $^2J_{H,H}$ = 13.1 Hz, 4H; *exo*-CH_2), 1.41 (s, 18H; $C(CH_3)_3$), 1.32 (s, 3H; tolyl-CH_3) 0.81 (s, 18H; $C(CH_3)_3$), 0.75 (s, 9H; $OC(CH_3)_3$), 0.70 ppm (s, 9H; $OC(CH_3)_3$); ^{13}C NMR ($CDCl_3$): δ = 151.34, 146.98, 132.37, 128.02, 125.62, 125.15, 124.82, 123.21, 63.46, 63.07, 34.24, 33.82, 31.64, 30.92, 26.64 ppm; ^{51}V NMR (C_6D_6): δ = −352.8 ppm ($\omega_{1/2}$ = 780 Hz); IR (cm^{-1}): $\tilde{\nu}$ = 3803w, 3582w, 3322bm, 3234m, 3079w, 3048w, 2962s, 2904s, 2867m, 2829w, 2388m, 2375w, 2361w, 2280s, 1864w, 1617s, 1484s, 1453s, 1433m, 1393m, 1362m, 1330s, 1299m, 1261m, 1242m, 1163m, 1123w, 1094s, 1010s, 944w, 872m, 812s, 753w, 730w, 702w, 665w; MS (E.S.): *m*/*z*: 927 [*M*−2×Me].

[{VCax(O)$_4$(NCMe)}$_2$]·6MeCN (8·6MeCN): [V(N*p*-tolyl)(O*n*Pr)$_3$] (1.0 g, 3.05 mmol) and calix[4]arene$(OH)_4$ (1.98 g, 3.05 mmol) were refluxed in toluene (30 mL) for 12 h. Volatiles were removed in vacuo, and the residue was extracted into hot MeCN (40 mL). Cooling to ambient temperature afforded yellow-orange prisms of **8** (184 mg, 5% yield). Elemental analysis calcd (%) for $C_{92}H_{112}N_2O_8V\cdot MeCN$: C 74.4, H 7.6, N 2.8; found: C 73.8, H 7.7, N 2.5. M.p. 185°C (decomp); ^{1}H NMR ($CDCl_3$) (sample dried in vacuo): δ = 7.83–6.95 (bm, 16H; Ar-*H*), 4.55–3.47 (broad features, 16H; CH_2), 1.39 (bs, 18H; $C(CH_3)_3$), 1.27 (bs, 18H; $C(CH_3)_3$), 1.19 ppm (bs, 36H; $C(CH_3)_3$); ^{13}C NMR ($CDCl_3$): δ = 146.83, 144.54, 127.82, 126.04, 113.39, 63.31, 32.56, 31.33, 1.99 ppm; ^{51}V NMR (C_6D_6): δ = −349.6 ppm ($\omega_{1/2}$ = 1200 Hz). μ_{eff} (Evans method, $C_6D_{12}/CDCl_3$, 298 K) = 1.36 μ_B; IR (cm^{-1}): $\tilde{\nu}$ = 3389bw, 2360s, 2330s, 1641w, 1454m, 1376w, 1260s, 1194m, 1092s, 1019s, 910w, 798s, 667m; MS (E.S.): *m*/*z*: 1475 [*M*$^+$], 1390.7 [*M*−2MeCN].

[{VCax(O)$_4$(NCMe)$_2$}$_2$]·MeCN (9) and [{VCax(O)$_4$(NCMe)$_2$}$_2$]·2MeCN (10): [$VCl_3(THF)_3$] (1.0 g, 2.68 mmol) and KO*t*Bu (0.93 g, 8.30 mmol) were combined in Et_2O (40 mL) at −78°C. After stirring for 6 h, volatiles were removed in vacuo, and calix[4]arene$(OH)_4$ (1.74 g, 2.68 mmol) in toluene (40 mL) was added and the system refluxed for 12 h. On cooling, volatile components were removed in vacuo, and the residue was extracted into hot MeCN (40 mL). Prolonged standing at ambient temperature (2–3 days) afforded both small red needles (**9**) in about 10% yield and thin orange plates (**10**) in about 25% yield.

[V(O)Cax(O)$_3$(OMe)(NCMe)]·2.5MeCN (11·2.5MeCN): [V(O)(O*n*Pr)$_3$] (3.61 mL, 15.91 mmol) and calix[4]arene$(OH)_3(OMe)$ (1.00 g, 1.50 mmol) were refluxed in toluene (30 mL) for 12 h. Following removal of volatiles in vacuo, the residue was extracted into MeCN (30 mL). Prolonged standing (1–2 days) at ambient temperature afforded **11** as red prisms (687 mg, 63% yield). Elemental analysis calcd (%) for $C_{45}H_{55}O_5V\cdot 2.5\,CH_3CN$: C 72.4, H 7.6, N 4.2; found: C 71.3, H 7.5, N 3.8; m.p. 185°C (decomp); ^{1}H NMR ($CDCl_3$): δ = 7.02 (s, 4H; Ar-*H*), 6.99 (s, 4H; Ar-*H*), 4.35 (d, $^2J_{H,H}$ = 12.8 Hz, 2H; *endo*-CH_2), 4.21 (s, 3H; $ArOCH_3$), 4.20 (d, $^2J_{H,H}$ = 12.8 Hz, 2H; *endo*-CH_2), 3.27 (d, $^2J_{H,H}$ = 12.8 Hz, 2H; *exo*-CH_2), 3.13 (d, $^2J_{H,H}$ = 12.8 Hz, 2H; *exo*-CH_2), 1.84 (s, 3H; CH_3CN), 1.20 (s, 18H; $C(CH_3)_3$), 1.13 ppm (s, 18H; $C(CH_3)_3$); ^{13}C NMR ($CDCl_3$): δ = 149.10, 146.50, 126.57, 124.70, 65.86, 65.66, 34.13, 31.47 ppm; ^{51}V NMR (C_6D_6, $CDCl_3$): δ: nothing seen in the range 2000 to −3000 ppm; IR (cm^{-1}): $\tilde{\nu}$ = 3160w, 2284w, 2245w, 1598w, 1461s, 1408w, 1377m, 1357m, 1301m, 1259m, 1196s, 1114m, 1014m, 990s, 942m, 921m, 867m, 826m, 798s, 755w; MS (E.S.): *m*/*z*: 726 [*M*$^+$].

[V(N*p*-tolyl)Cax(O)$_3$(OMe)(NCMe)]·1.125MeCN (12·1.125MeCN): [V(N*p*-tolyl)(OEt)$_3$] (2.30 g, 8.03 mmol) and calix[4]arene$(OH)_3(OMe)$ (0.50 g, 0.75 mmol) were refluxed in toluene (30 mL) for 12 h. Following removal of volatiles in vacuo, the residue was extracted into MeCN (30 mL). Prolonged standing (1–2 days) at ambient temperature afforded **12** as red-brown prisms (816 mg, 40% yield). Elemental analysis calcd (%) for $C_{52}H_{62}NO_4V\cdot MeCN$: C 75.7, H 7.6 N 3.3; found: C 74.5, H 7.7, N 2.7; m.p. 185°C (decomp); ^{1}H NMR ($CDCl_3$): δ = 7.43 (d, $^3J_{H,H}$ = 8.3 Hz, 2H; tolyl-*H*), 7.27 (d, $^3J_{H,H}$ = 8.3 Hz, 2H; tolyl-*H*), 7.21 (d, $^4J_{H,H}$ = 2.7 Hz, 2H; Ar-*H*), 7.19 (d, $^4J_{H,H}$ = 2.7 Hz, 2H; Ar-*H*), 4.70 (d, $^2J_{H,H}$ = 12.9 Hz, 2H; *endo*-CH_2), 4.40 (d, $^2J_{H,H}$ = 12.6 Hz, 2H; *endo*-CH_2), 4.34 (s, 3H; OCH_3), 3.40 (d, $^2J_{H,H}$ = 12.9 Hz, 2H; *exo*-CH_2), 3.30 (d, $^2J_{H,H}$ = 12.6 Hz, 2H; *exo*-CH_2), 2.50 (s, 3H; tolyl-CH_3), 1.92 (s, 3H; CH_3CN), 1.14 (s, 18H; $C(CH_3)_3$), 1.35 ppm (s, 18H; $C(CH_3)_3$); ^{13}C NMR ($CDCl_3$): δ = 160.44, 145.41, 144.91, 138.73, 129.09, 128.42, 127.75, 124.69, 124.27, 66.12, 65.80, 34.13, 31.55, 21.30 ppm; ^{51}V NMR (C_6D_6): δ = −322.6 ppm ($\omega_{1/2}$ = 925 Hz); IR (cm^{-1}): $\tilde{\nu}$ = 3153w, 3052w, 3021w, 2964s, 2904s, 2868m, 2358w, 2344w, 2252m, 1782w, 1588w, 1478s, 1460s, 1435m, 1414m, 1393m, 1362m, 1301m, 1261s, 1201s, 1167w, 1093s, 1011s, 944m, 908s, 875m, 800s, 733s, 679w, 667m, 650s; MS (E.S.): *m*/*z*: 815 [*M*$^+$].

[{VOCax(O)$_4$}$_2$(μ-2,6-(CH$_2$)$_2$C$_5$H$_3$N)]·4MeCN (13·4MeCN): [$VOCl_3$] (0.13 mL, 1.40 mmol) and [Cax(OH)$_2$(μ-OpyO)]$_2$ (1.00 g, 0.67 mmol) were refluxed in toluene (50 mL) for 12 h. Following the removals of volatiles in vacuo, the residue was extracted into hot dichloromethane (30 mL). Prolonged standing (1–2 days) at ambient temperature afforded brown prisms of **13** (0.05 g, 5% yield), further product can be obtained from the mother-liquor (0.31 g, 30% total yield). Elemental analysis calcd (%) for $C_{95}H_{111}NO_{10}V_2\cdot 1.5\,CH_2Cl_2$: C 70.0, H 6.9, N 0.9; found: C 69.6, H 7.0, N 0.7; m.p. 186°C (decomp); ^{1}H (C_6D_6): δ = 8.01 (d, $^3J_{H,H}$ = 7.29 Hz, 2H; 3,5-C_5H_5N), 7.31 (s, 1H; 4-C_5H_3N), 7.29–6.93 (m, 16H; Ar-*H*), 5.54 (s, 4H; CH_2), 4.76 (d, $^2J_{H,H}$ = 13.0 Hz, 4H; *endo*-CH_2), 4.45 (d, $^2J_{H,H}$ = 13.0 Hz, 4H; *endo*-CH_2), 3.18 (d, $^2J_{H,H}$ = 13.0 Hz, 8H; *exo*-CH_2), 0.86 (s, 36H; $C(CH_3)_3$), 0.82 ppm (s, 36H; $C(CH_3)_3$); ^{13}C NMR ($CDCl_3$): δ = 150.56, 146.68, 145.81, 127.77, 126.01, 123.77, 121.22, 68.20, 63.32, 34.20, 31.42 ppm; ^{51}V NMR (C_6D_6): δ = −371.5 ppm ($\omega_{1/2}$ = 2170 Hz); IR (cm^{-1}): $\tilde{\nu}$ = 3316w, 3269w, 3231m, 3075w, 3044w, 2955m, 2924m, 2854m, 2609w, 2520w, 2384m, 2372m, 2357m, 2275s, 1988w, 1902w, 1864w, 1615m, 1545w, 1448s, 1386w, 1332s, 1258s, 1192m, 1157m, 1095s, 1013s, 943w, 866w, 807s, 730w, 664m; MS (E.S.): *m*/*z*: 1528 [*M*$^+$].

X-ray crystallography: Crystal data were collected on a Bruker SMART 1000 CCD diffractometer using narrow slice 0.3° ω-scans for **1a**, **2**, **4**, **6**–**8**, and **13**. Data for **1b**, **5**, **9**, **10**, **11**, **12**, were collected at Daresbury Laboratory SRS Station 9.8 (16.2 SMX for **5**) using silicon 111 monchromated X-radiation. Data for **3** were collected on an Enraf Nonius KappaCCD diffractometer equipped with a rotating anode source and using ω and ϕ scans and wide slices. Data were corrected for Lp effects and for absorption, based on repeated and symmetry equivalent reflections, and solved by direct methods (Patterson synthesis for **10**). Structures were refined by full matrix least squares on F^2. H atoms were included in a riding model. Hydrogen atom U_{iso} values were constrained to be 120% of that of the carrier atom except for methyl-H (150%). Several structures (**1a**, **2**–**5**, **10**–**13**), exhibited disorder in the *t*Bu groups. This disorder was modelled with two sets of methyl carbon positions with restraints on geometry and anisotropic displacement parameters. In **8** a *t*Bu group was disordered with two methyl groups common and two sets of positions for the tertiary carbon and the remaining methyl carbon. In **12** there are four molecules in the asymmetric unit. Neighbouring pairs of molecules exhibit disorder of the methyl groups of the OMe moieties, while one of the four molecules has a disordered *p*-tolyl imido group in which the nitrogen and *ipso*-carbon atoms are common, but the remainder are split over two sets of positions. MeCN molecules of crystallisation were also often disordered and where necessary were either modelled over two sets of positions or as partially occupied. The formula of **5** includes one badly disordered, MeCN molecule that was modelled as a region of diffuse electron density by the Platon "Squeeze" procedure.[33]

Programs used: Bruker SMART and Enraf Nonius COLLECT (data collection), Bruker SAINT and DENZO (integration & cell refinement), and SHELXTL (solution, refinement and graphics), and local programs. CCDC-240185–240187 and CCDC-298824–298834 contain the supplementary crystallographic data for **1a,b** and **2** and **3**–**13**, respectively. These data can be obtained free of charge from The Cambridge Crystallographic Data Centre via www.ccdc.cam.ac.uk/data_request/cif.

Acknowledgements

We would like to thank the National Mass Spectrometry Service (Swansea, UK), the EPSRC for studentships to L.W., M.A.R., D.M.H. and S.H.D., and for the award of beam-time at Daresbury Laboratory. The Royal Society and the EPSRC (INTERACT Japan programme) are thanked for financial support, and the EPSRC UK National Crystallography Service at Southampton is thanked for data collection for **3**. Dr. Myles Cheesman (UEA) is thanked for help with EPR experiments.

[1] F. Cadogen, K. Nolan, D. Diamond in *Calixarenes 2001* (Eds.: Z. Asfari, V. Böhmer, J. Harrowfield, J. Vicens), Kluwer Academic Publishers, Dordrecht, **2001**.

[2] a) Y.-S Zheng, L.-Q Ying, Z.-Q Shen, *Polymer* **2000**, *41*, 1641; b) J. Ling, Z. Shen, W. Zhu, *J. Polym. Sci. A* **2003**, *41*, 1390; c) O. V. Ozerov, N. P. Rath, F. T. Ladipo, *J. Organomet. Chem.* **1999**, *586*, 223; d) C. Capacchione, P. Neri, A. Proto, *Inorg. Chem. Commun.* **2003**, *6*, 339; e) Y. Chen, Y. Zhang, Z. Shen, R. Kou, L. Chen, *Eur. Polym. J.* **2001**, *37*, 1181; f) V. C. Gibson, C. Redshaw, M. R. J. Elsegood, *J. Chem. Soc. Dalton Trans.* **2001**, 767; g) C. Huang, J. Ahn, S. Kwon, J. Kim, J. Lee, Y. Han, H. Kim, *Applied Cat. A* **2004**, *258*, 173; h) L. Giannini, A. Caselli, E. Solari, C. Floriani, A. Chiesi-Villa, C. Rizzoli, N. Re, A. Sgamellotti, *J. Am. Chem. Soc.* **1997**, *119*, 9198; i) R. A. Kemp, D. S. Brown, M. Lattman, J. Li, *J. Mol. Catal. A* **1999**, *149*, 125.

[3] a) A. Diaz-Barrios, J. Liscano, M. Trujillo, G. Agrifoglio, J. O. Matos, **1997**, EP 97–201629; b) J. J. Ha, Y. H. Han, C. Z. Huang, H. R. Kim, J. S. Kim, J. S. Kim, J. H. Lee, G. S. Song, **2003**, KR 2003037474; c) S. Nagy **2004**, US 2004214715.

[4] a) C. D. Gutsche, *Calixarenes*, Royal Society of Chemistry, Cambridge, **1989**; b) D. M. Roundhill, *Prog. Inorg. Chem.* **1995**, *43*, 553; c) C. Wieser, C. B. Dielman, D. Matt, *Coord. Chem. Rev.* **1997**, *165*, 93; d) A. Ikeda, S. Shinkai, *Chem. Rev.* **1997**, *97*, 1713; e) C. D. Gutsche, *Calixarenes Revisited*, Royal Society of Chemistry, Letchworth, **1988**; f) C. Floriani, R. Floriani-Moro, *Adv. Organomet. Chem.* **2001**, *47*, 167; g) W. Sliwa, *Croat. Chem. Acta* **2002**, *74*, 131; h) P. D. Harvey, *Coord. Chem. Rev.* **2002**, *233/234*, 289; i) C. Redshaw, *Coord. Chem. Rev.* **2003**, *244*, 45; j) F. A. Cotton, L. M. Daniels, C. Lin, C. A. Murrillo, *Inorg. Chim. Acta* **2003**, *347*, 1; k) A. J. Petrella, C. L. Raston, *J. Organomet. Chem.* **2004**, *689*, 4125.

[5] a) P. D. Hampton, C. E. Daitch, T. M. Alam, Z. Becze, M. Rosay, *Inorg. Chem.* **1994**, *33*, 4750; b) P. D. Hampton, C. E. Daitch, T. M. Alam, Z. Becze, M. Rosay, *Inorg. Chem.* **1997**, *36*, 2879; c) B. Masci in *Calixarenes 2001*, (Eds.: Z. Asfari, V. Böhmer, J. Harrowfield, J. Vicens, Kluwer Academic Publishers, **2001**, Chapter 12.

[6] a) D. Reardon, J. Guan, S. Gambarotta, G. P. A. Yap, D. R. Wilson, *Organometallics* **2002**, *21*, 4390; b) K. Nomura, A. Sagara, Y. Imanishi, *Macromolecules* **2002**, *35*, 1583; c) K. Takaoki, T. Miyatake, *Macromol. Symp.* **2000**, *157*, 251.

[7] a) See for example: M. P. McDaniel, K. S. Collins, A. P. Eaton, E. A. Benham, J. L. Martin, M. D. Jensen, G. R. Hawley, **1999**, U. S. Patent No. 6391816; b) M. Arndt-Rosenau, M. Hoch, J. Sundermeyer, J. Kipke, X. Li, **2003**, U. S. Patent No. 2003/0130451.

[8] a) K. Nomura, A. Sagara, Y. Imanishi, *Chem. Lett.* **2001**, 38; b) W. Wang, J. Yamada, M. Fujiki, K. Nomura, *Catal. Commun.* **2003**, *4*, 159; c) Y. Nakayama, H. Bando, Y. Sonobe, Y. Suzuki, T. Fujita, *Chem. Lett.* **2003**, *32*, 766; d) Y. Nakayama, H. Bando, Y. Sonobe, T. Fujita, *J. Mol. Catal. A* **2004**, *213*, 141; e) Y. Nakayama, H. Bando, Y. Sonobe, T. Fujita, *Bull. Chem. Soc. Jpn.* **2004**, *77*, 617; f) C. Redshaw, L. Warford, M. R. J. Elsegood, S. H. Dale, *Chem. Commun.* **2004**, 1954; g) C. Redshaw, **2004**, U.K. Patent No. 0403984.8; h) A. K. Tomov, V. C. Gibson, D. Zaher, M. R. J. Elsegood, S. H. Dale, *Chem. Commun.* **2004**, 1956; i) W. Wang, K. Nomura, *Macromolecules* **2005**, *38*, 5905.

[9] F. H. Allen, *Acta Crystallogr. Sect. B* **2002**, *58*, 380. A search of the CSD (v.5.27 + 1 update, Jan 2006) produced 4091 examples with a mean V=O distance of 1.61 Å (range 1.431–2.477 Å, SD 0.070).

[10] a) W. Clegg, M. R. J. Elsegood, S. J. Teat, C. Redshaw, V. C. Gibson, *J. Chem. Soc. Dalton Trans.* **1998**, 3037; b) W. Clegg, *J. Chem. Soc. Dalton Trans.* **2000**, 3223.

[11] D. D. Devore, J. D. Lichtenhan, F. Takusagawa, E. A. Maatta, *J. Am. Chem. Soc.* **1987**, *109*, 7408.

[12] K. Suzuki, H. Minami, Y. Yamagata, S. Fujii, K. Tomita, Z. Asfari, J. Vicens, *Acta Crystallogr. Sect. C* **1992**, *48*, 350.

[13] a) B. Castellano, E. Solari, C. Floriani, N. Re, A. Chiesi-Villa, C. Rizzoli, *Organometallics* **1998**, *17*, 2328; b) B. Castellano, E. Solari, C. Floriani, R. Scopelliti, N. Re, *Inorg. Chem.* **1999**, *38*, 3406; c) E. Hoppe, C. Limberg, B. Ziemer, C. Mügge, *J. Mol. Catal. A* **2006**, *251*, 34.

[14] a) V. C. Gibson, T. P. Kee, A. Shaw, *Polyhedron* **1988**, *7*, 579; b) Y. Takashima, Y. Nakayama, H. Yasuda, A. Harada, *J. Organomet. Chem.* **2002**, *651*, 114.

[15] E. D. Gueneau, K. M. Fromm, H. Goesmann, *Chem. Eur. J.* **2003**, *9*, 509.

[16] a) J. J. H. Edema, S. Gambarotta, F. van Bolhuis, A. L. Spek, *J. Am. Chem. Soc.* **1989**, *111*, 2142; b) J. J. H. Edema, S. Gambarotta, F. van Bolhuis, W. J. J. Smeets, A. L. Spek, *Inorg. Chem.* **1989**, *28*, 1407; c) J. J. H. Edema, A. Meetsma, S. Gambarotta, S. I. Khan, W. J. J. Smeets, A. L. Spek, *Inorg. Chem.* **1991**, *30*, 3639.

[17] D. J. MacDougall, J. J. Morris, B. C. Noll, K. W. Henderson, *Chem. Commun.* **2005**, 456.

[18] U. Radius, *Z. Anorg. Allg. Chem.* **2004**, *630*, 957.

[19] See for example: F. Wolff, C. Lorber, R. Choukroun, B. Donnadieu, *Eur. J. Inorg. Chem.* **2004**, 2861, and references therein.

[20] H. Ross, U. Lüning, *Angew. Chem.* **1995**, *107*, 2723; *Angew. Chem. Int. Ed. Engl.* **1995**, *34*, 2555.

[21] a) D. C. Crams, P. K. Shin, *J. Am. Chem. Soc.* **1994**, *116*, 1305; b) H. Hagen, C. Bezemer, J. Boersma, H. Kooijman, M. Lutz, A. L. Spek, G. van Koten, *Inorg. Chem.* **2000**, *39*, 3970.

[22] R. A. Henderson, D. L. Hughes, Z. Janas, R. L. Richards, P. Sobota, S. Szafert, *J. Organomet. Chem.* **1998**, *554*, 195.
[23] M. Arndt-Rosenau, M. Hoch, J. Sundermeyer, J. Kipke, X. Li, **2003**, United States Patent No. US 2003/0130451 A1.
[24] S. Gambarotta, *Coord. Chem. Rev.* **2003**, *237*, 229.
[25] Y. Ma, D. Reardon, S. Gambarotta, G. Yap, H. Zahalka, C. Lemay, *Organometallics* **1999**, *18*, 2773.
[26] G. S. Long, B. Snedeker, K. Bartosh, M. L. Werner, A. Sen, *Can. J. Chem.* **2001**, *79*, 1026.
[27] M. Tanabiki, K. Tsuchiya, Y. Motoyama, H. Nagashima, *Chem. Commun.* **2005**, 3409.
[28] a) G. J. P. Britovsek, V. C. Gibson, D. F. Wass, *Angew. Chem.* **1999**, *111*, 448; *Angew. Chem. Int. Ed.* **1999**, *38*, 428; b) V. C. Gibson, S. K. Spitzmesser, *Chem. Rev.* **2003**, *103*, 283; c) V. C. Gibson, E. L. Marshall in *Comprehensive Coordination Chemistry II, vol 9* (Eds.: J. A. McCleverty, T. J. Meyer, M. D. Ward), Elsevier, **2004**.
[29] a) A. G. Evans, J. C. Evans, E. H. Moon, *J. Chem. Soc. Dalton Trans.* **1974**, 2390; b) A. G. Evans, J. C. Evans, J. Mortimer, *J. Am. Chem. Soc.* **1979**, *101*, 3204.
[30] M. Lutz, H. Hagen, A. M. M. Schreurs, A. L. Spek, G. van Koten, *Acta Crystallogr. Sect. C* **1999**, *55*, 1636.
[31] E. Kurras, *Naturwissenschaften* **1959**, *46*, 171.
[32] a) A. Arduini, A. Casnati in *Macrocycle Synthesis* (Ed.: D. Parker), Oxford University Press, New York, **1996**, chapter 7; b) A. Zanotti-Gerosa, E. Solari, L. Giannini, C. Floriani, N. Re, A. Chiesi-Villa, C. Rizzoli, *Inorg. Chim. Acta* **1998**, *270*, 298.
[33] A. L. Spek, *Acta Crystallogr. A* **1999**, *46*, C34.
[34] Note added in proof (November 2, 2006): Limberg et al. have recently published the complex $[\{VO(OMe)\}_2(\mu\text{-}O)Cax(OMe)_2(O)_2]$, the structure of which resembles that of **4** and **5** presented herein. See E. Hoppe, C. Limberg, B. Ziemer, *Inorg. Chem.* **2006**, *45*, 8308

Received: May 16, 2006
Published online: November 20, 2006

